sustainability

MDPI

Article

Solar Species: Energy Optimization of Urban Form Through an Evolutionary Design Process

Simone Giostra [1], Ayush Kamalia [2] and Gabriele Masera [2,*]

[1] Department of Architecture and Urban Studies, Politecnico di Milano, 20133 Milan, Italy; simone.giostra@polimi.it
[2] Department of Architecture, Built Environment and Construction Engineering, Politecnico di Milano, Via Ponzio 31, 20133 Milan, Italy; ayush.kamalia@mail.polimi.it
* Correspondence: gabriele.masera@polimi.it

Abstract: This paper proposes design guidelines to enhance energy efficiency and energy generation potential in active solar buildings. Additionally, it presents a variety of optimized urban forms characterized by attributes such as shape, layout, and number of buildings on the plot. These urban configurations are classified into solar species, each associated with a distinct range of high passive and active solar potential. These results were achieved by developing and applying a simulation-driven, multi-objective optimization technique for the early-stage design of a residential building cluster in a temperate climate. This method leverages both passive and active energy indicators, employing a genetic algorithm to identify optimal forms that maximize active solar potential while also minimizing operational energy demand. The approach utilizes a parametric modelling routine that relies on vertical cores and horizontal connections to produce design iterations featuring irregular geometry, while ensuring structural continuity and means of egress. The findings reveal a significant variability in onsite energy generation, with optimized solutions differing by a factor of 2.5 solely based on shape, underscoring the critical role of active solar potential. Taken together, these results hint at the descriptive and predictive capabilities of these solar species, making them a promising heuristic model for characterizing urban form in relation to energy performance.

Keywords: active energy buildings; early-stage design; energy form-finding; genetic algorithms; multi-objective optimization

Citation: Giostra, S.; Kamalia, A.; Masera, G. Solar Species: Energy Optimization of Urban Form Through an Evolutionary Design Process. *Sustainability* **2024**, *16*, 9254. https://doi.org/10.3390/su16219254

Academic Editors: Patrick Dallasega, Monika Siewczyńska, Piotr Nowotarski and Maria Ratajczak

Received: 13 September 2024
Revised: 16 October 2024
Accepted: 21 October 2024
Published: 24 October 2024

1. Introduction

1.1. Context

For centuries, architects have relied on heuristic design methods, such as building typologies, aesthetic canons, or rules of thumb, to ensure adequate levels of comfort and safety in buildings. More recently, countless design manuals have promoted a normative design practice based on codes and regulations, starting with standardization efforts by Ernst Neufert [1]. Over the same period, the building sector has witnessed a continuous increase in energy consumption, particularly following the widespread adoption of electricity and fossil fuels for heating, cooling, and lighting in the early 20th century [2]. Despite the design profession's growing interest in passive design principles and renewable energy sources, spurred by the energy crisis in the 1970s, energy consumption in buildings has continued to grow [3].

Today, the architecture, engineering, and construction (AEC) sector is accountable for 40% of energy consumption and nearly 36% of CO_2 emissions in the EU [4], with half of the building energy usage related to heating, ventilation, and air conditioning (HVAC) systems [5]. AEC is considered one of the most cost-effective sectors for climate action [6] and the European Union has set ambitious targets for retrofits and new construction, with the aim of achieving a "highly efficient and decarbonized building stock by 2050" [7].

In response to new and more stringent regulations, architects are gradually embracing a growing range of building simulation tools to meet increasingly demanding energy and emission targets [8,9]. Automated design methods, developed over the past two decades, present opportunities to generate, simulate, and optimize design solutions aimed at reducing energy consumption, GHG emissions, and environmental impact [10].

1.2. Need

Despite recent advances, these digital design tools and methods remain too complex and time-consuming to use, particularly at the conceptual phase of design. Additionally, existing computational design methods driven by energy-related goals often overlook critical structural and safety considerations. Consequently, many architects continue to rely on design guidelines, experience, and intuition to make decisions that potentially compromise the energy-saving potential of their projects [11]. Energy calculations typically occur late in the design process as a way of generating reports for compliance with mandatory energy regulation requirements [12]. Similarly, mechanical systems and insulation materials are often retroactively applied to mitigate the adverse effects of poorly informed design decisions made by traditional means earlier in the process [13]. Paradoxically, stricter standards aimed at reducing operational energy use can inadvertently increase the embodied energy in construction, maintenance, and decommissioning [14]. By and large, the vast glass surfaces, paper-thin enclosures, and prominent structural forms of the modernist aesthetic—plus the convoluted geometries facilitated by computational design tools—remain a prevailing style in architecture today. Without implementing additional measures to bolster energy efficiency and decarbonize energy supply, the building sector will not be able to meet the zero-carbon objective by 2050, nor the interim milestone set for 2030 [15].

1.3. Task

This paper aims at identifying optimal forms and layouts for a residential building cluster situated in a temperate climate, deploying a simulation-driven, multi-objective optimization method based on passive and active energy indicators. The primary objective is to minimize operational energy consumption while simultaneously maximizing onsite energy generation potential. This research underscores the significance of early-stage design as the "low-hanging-fruit" of optimization in buildings when decisions carry the greatest potential for energy savings. Moreover, during this phase, design variables hold the most relevance for architects, focusing predominantly on geometry rather than materials or building systems. This study tackles current limitations in automated design methods by enhancing three key aspects of the optimization process:

1. Core key objectives: We optimize towards only two objectives, intended to encapsulate the dual mandates of EU energy legislation—low energy consumption and a high onsite energy fraction.
2. Easy-to-compute indicators: our approach relies on computationally friendly yet reliable metrics to streamline and broaden the search during the initial optimization phase. Subsequent full-climate simulation, conducted on the best-performing solutions identified by this method, largely validate the selected indicators as dependable proxies for energy production and savings potential in buildings.
3. Viable design variants: the optimization process focuses on geometric variables related to building massing that are easy to iterate yet are central to a conceptual design process in architecture. The resulting parametric modelling routine generates a diverse range of irregular building shapes, all structurally viable and compliant with egress requirements.

1.4. Outcomes

The research outcomes are poised to advance knowledge in three areas of energy-driven design practice, offering potential applications in the immediate, short, and medium term, respectively:

1. Design Guidelines: This paper identifies patterns of causal relationship between geometrical forms and energy performance in buildings; it also arrives at a final ranking of optimal solutions based on total energy use, including passive and active contributions. The results should provide useful design guidelines in the early phase of design, at least until automated design methods become more accessible to a wider range of architects.
2. Optimization Workflow: The design process outlined in this paper can be tailored to project-specific requirements such as program, context, or climate. Our proposed workflow offers practitioners a viable method of algorithm-based design, particularly as processing times are expected to decrease with the advent of parallel or cloud computing in the near future.
3. Training Dataset: A synthetic dataset encompassing environmental performance data for over 20,000 buildings can serve as a valuable resource for training neural networks in the next phase of the project, eventually leading to a new generation of automated design tools.

Ultimately, this research aims to complement traditional heuristic methods of architectural design with the blind yet powerful creative mechanisms of biological natural selection. The use of genetic algorithms should help architects moving beyond the energy-intensive forms of modernism and toward the yet-unexplored, low-carbon forms of solar species that are needed for reversing the current trajectory of energy use in buildings.

2. Background

2.1. Building Performance Simulation (BPS)

Shape and orientation [16], along with thermal properties and storage capacity of the envelope [17], play pivotal roles in the energy performance of buildings. Factors such as shading and fenestration [18], including window type, location, and size [19], and occupants' behavior and lifestyle further influence the availability of daylighting, natural ventilation, direct and indirect solar heat gains, while also affecting heat loss [20]. Latitude and climate introduce additional variability to this intricate balance. Consequently, these elements collectively impact the demand for artificial lighting and the heating and cooling loads in buildings. In addition to passive design strategies, the integration of active systems such as solar thermal and photovoltaic technology to produce hot water and electricity, sometimes integrated with solar shading to reduce heat gains and to control glare, can significantly alter the overall energy balance of the building. Due to the intricate and sometimes conflicting effects of countless design variables on energy performance objectives, architects increasingly turn to building performance simulation (BPS) tools to anticipate and assess the energy consequences of various design alternatives [21]. Dynamic simulation tools for complex thermal modeling and energy behavior, for example, offer a detailed evaluation of different end-uses, such as heating, cooling, and lighting, and allow architects to identify areas of potential improvement.

Today, the seamless integration of performance assessment tools throughout the design process is considered a key factor for improving the energy efficiency and the life cycle emissions in buildings [22]. While a plethora of building energy simulation engines exist for design professionals, with TRNSYS and EnergyPlus among the most common simulators [23], supported by over 200 interfaces and applications for EnergyPlus alone [24], their utilization remains laborious and demands specialized expertise. Moreover, most tools operate as "black boxes" with limited user engagement [25] and do not provide actionable insights on how energy performance relates to specific building geometry, components, or materials. As a result, BPS tools primarily serve to evaluate and compare a few design options, often relying on a limited number of variables or simplified indicators in a trial-and-error process, rather than to pro-actively guide toward optimal design solutions. The use of energy modeling tools, for example, is often limited to simulating the thermal energy demand of the building [26]. Alternatively, BPS tools have been utilized for sensitivity analysis of individual design parameters and components, such as insulation material

type and thickness [27], or size and orientation of sun-shading devices [28]. Sensitivity analyses, however, typically optimize parameters in isolation, neglecting the intricate interplay between variables and the potential energy savings resulting from exploring these interactions. The complex behavior of buildings, influenced by shape and orientation, size, angle and location of windows and related shading components, as well as reflectivity and thermal properties of the envelope, transcends the sum of individual components considered in isolation [29]. On the other hand, tools that attempt to capture the complex behavior of interrelated factors such as building geometry, materials, and systems, while producing reliable and readily available outcomes, can only operate on a single or a limited number of design options.

2.2. Architectural Design Optimization (ADO)

The complexity and computational cost associated to evaluating myriad variables, which can result in a vast number of valid design variants, requires the use of optimization methods to explore the solution space more efficiently and faster. In architectural design optimization (ADO), building performance simulation tools like EnergyPlus are coupled with automated optimization routines to assess a broader spectrum of options, often generated by parametric modelling facilitated by tools like Grasshopper [30] and related plug-ins. In this approach, the simulation program computes the objective function, while an optimization algorithm manipulates the design variables iteratively, generating a pool of alternatives with the aim of identifying optimal solutions that meet all constraints [23]. The purpose of using optimization algorithms is to reduce the number of simulations by searching for progressively better approximations to a solution. The concept of employing mathematical models for design optimization dates back to Gupta's work in 1970, which focused on enhancing thermal comfort and reducing heating and cooling loads in buildings [31]. The field has expanded dramatically since the early 2000s [23], for example with research by Caldas and Norford [32] on optimizing window location and sizing in office buildings to minimize lighting, heating, and cooling loads.

Recent advances in optimization theory and increasing the availability of cloud computing make the use of algorithmic optimization a highly promising method in designing high-performance buildings, with genetic algorithms (GAs) and particle swarm optimization emerging as the most utilized in architecture [33]. A GA is a population-based algorithm that emulates the iterative process of biological evolution by selecting the fittest individuals from each generation to produce subsequent generations, gradually converging on optimal solutions [34]. The foundation of machine learning rooted in evolutionary mechanisms, including mutation and recombination, was laid by John Holland in 1975 [35]. In this process, recombination typically generates new individuals from existing genetic material with high fitness, while mutation extends the search to unexplored regions of the fitness landscape. A GA proves particularly effective in navigating large and discontinuous search spaces, where identifying the best solution incurs substantial costs, and near-optimal solutions suffice. Today, genetic optimization techniques find routine application across a diverse spectrum of objective functions in architecture [36], including energy consumption [37], thermal and visual comfort [38], economic considerations [39], air quality, carbon emissions [40], and even aesthetics [41], leading to optimized urban layout [42], building shapes [43], and energy systems [44], with facades as the most frequent optimization target [45]. Despite its widespread adoption in design optimization, GA still presents notable challenges. For instance, it requires evaluating a sizable pool of iterations that may not yield near-optimal solutions [46]. Further, detailed evaluation of individual solutions can prove computationally intensive, especially when dealing with simulations employing ray-tracing methods.

2.3. Parametric Modelling

Parametric modelling of design variants is another area of research witnessing rapid progress. These variants are typically obtained by iterating geometric parameters such as height, width, and length of a base volume, using step intervals related to typical floor-

to-floor distance and structural modules. When dealing with multiple buildings, some methods may also incorporate considerations like minimum distances between volumes, setbacks from plot edges, and courtyard widths. The starting volume is often a regular building with a rectangular footprint: for instance, Giostra, Masera, and Monteiro [47] explored three base typologies (bar, tower, and courtyard) generating 312 building shapes for a sensitivity analysis of form and orientation in relation to active and passive solar potential indicators.

Some studies introduce additional typologies with L-shape, T-shape, H-shape, and U-shape footprints, using shape parameters [48], such as aspect ratio, window-to-wall ratio, or area-to-volume ratio [49] to generate design variants. In these and other cases, the formal and organizational traits of the originating typology guarantee viable models while also limiting the range of variants explorable by the optimization process to predictable building forms [50]. Some researchers attempt to mitigate these limitations by introducing additional parameters, such as varying the angles between walls [51]. Adding geometric variables, however, significantly increases the pool of potential design variants, prompting the introduction of further constraints, for example by restricting the footprint of the building to a four-sided courtyard in the previous study, for a total of only 256 forms. Conversely, an increasing number of parametric modeling methods and tools can generate higher topological variability, producing 'out-of-the-box' solutions. However, these solutions often suffer from practical limitations such as structural integrity, horizontal and vertical accessibility, or compliance with minimum daylight and natural ventilation requirements, rendering them impractical or unbuildable.

The Grasshopper plugin EvoMass [52], for instance, generates building massing options through an early-stage, performance-based single objective design optimization algorithm, employing either subtractive or additive generation principles [53]. This method emulates manual building massing techniques traditionally utilized in the conceptual phase of design, such as incorporating building blocks or carving voids into physical models, thus offering a more intuitive process for architects. A broader range of geometric variability, however, comes at the cost of limiting the search to a single objective function. The parametric modeling also overlooks structural continuity and the minimum distance between volumes, potentially yielding solutions that do not adhere to building codes or gravitational constraints. Additionally, built-in design rules and constraints, such as requirements for a minimum lot coverage or a single building volume, may prove arbitrary.

The aggregation of discreet elements, often called voxels, serves as the basis for various design tools and methodologies. Luca and Sepúlveda [54], for instance, develop a workflow based on the solar envelope principle [55] to mitigate the impact of new construction on existing buildings, especially in dense urban areas. Their study subdivides the maximum allowable building volume into 'space voxels', which are then analyzed for their effect on the solar access of neighboring buildings. The new building form is generated by removing voxels that obstruct the windows of neighboring facades, while voxels with neutral or positive effects remain in place.

These voxel-based tools using aggregative or subtractive methods, however, often overlook the adverse effects of mutual obstruction among voxels, as well as performance targets related to building interiors, in order to reduce computational costs. Voxel aggregations are also inherently prone to structural discontinuity and a significant increase in building envelope area, potentially leading to higher heating and cooling loads.

2.4. Multi-Objective Optimization (MOO)

The interrelated and often conflicting effects of design variables on various performance targets prompt the adoption of multi-objective optimization (MOO) algorithms, enabling the consideration of multiple performance targets simultaneously [56]. This approach proves particularly effective when facing conflicting objectives that must be minimized or maximized concurrently. Large glazing can positively affect daylighting and heat gains in winter, for example, while also increasing the risk of glare and cooling loads in summer. MOO generates a set of solutions displayed in an n-dimensional space, depending

on the number of objectives, with optimal outcomes approximating trade-off curves known as Pareto fronts, for which an objective cannot be improved without compromising others. While early optimization efforts were primarily focused on single objectives, an increasing number of building optimization studies now address two or more objectives [56], with over 40% of papers included in a recent review employing MOO [45].

Numerous studies explore multi-objective optimization with the use of GA. For instance, Gagne and Andersen [57] investigate optimal facade configurations for improved illuminance and glare during the early design phase, while Carlucci et al. [58] focused on multi-objective optimization towards nearly zero-energy buildings, and Jafari and Valentin [59] on the selection of objective functions in energy retrofits. More recently, Ascione et al. [60] introduced Harlequin, a comprehensive framework for the MOO of building energy design, while Gou et al. [61] examined multi-family apartment buildings in China. Today, MOO methods prove best suited to address the escalating demands of energy regulations and certification schemes such as LEED [62], requiring the concurrent evaluation of up to 100 design objectives. Yet, despite the potential of multi-objective, performance-driven building optimization, its integration into architectural practice remains limited [63]. Various authors cite barriers including time-consuming computations [64], particularly with high-dimensional optimization problems [46], and the challenges optimization algorithms face in handling uncertainties [56]. MOO requires specialized knowledge in properly defining the design problem, selecting, and running the software, and integrating optimization tools with simulation engines.

Among practitioners using visual programming platforms for optimizing the building geometry based on energy indicators, a majority identify speed of convergence, formulating the optimization problem, and understanding the results as primary challenges in a survey of 186 users [65]. These findings align with earlier observations by Nault et al. [50] while conducting a workshop on their "UrbanSOLVE" optimization tool. As a result, there are few, if any, tools that enable designers to compare and rank a meaningful number of design variants based on multiple performance targets, with speed and usability required by a typical building design process [66].

2.5. Early Design Phase

The challenges in usability are particularly critical in the early design phase, when the substantial computational time required to assess numerous design variables clashes with the need for rapid exploration of ideas at the conceptual stage [67]. In fact, recent surveys [68] indicate that only a small fraction of the 400 building simulation tools listed by the U.S. Department of Energy are tailored for early design deployment.

Yet, the potential for energy savings during the concept design stage is extensively documented in the literature [33]. For instance, studies by Baker and Steemers [69] demonstrate that early design considerations could lead to variations in energy demand by a factor of 2.5, while optimizing building shape and orientation could reduce energy demand by up to 40% at comparable costs [70]. Conversely, adverse decisions made in the early design phase can have a disproportionate impact on final performance [13], effectively setting a ceiling on the active and passive solar potential of subsequent design choices. Factors such as shape and orientation, for example, significantly influence daylighting, solar radiation intake, and the potential for energy generation using photovoltaic and solar thermal systems [71]. Moreover, early decisions can severely constrain the design space, making it more challenging or expensive to achieve energy targets later in the process. Hence, the current study focuses on building massing as the phase of design with the most significant impact on building energy use—an arena ripe with "low hanging fruit" for optimization efforts in architecture.

3. Methodology

3.1. Overview: Objectives, Indicators, Design Variables

The research presented here aims to uncover optimal forms and layouts for a residential building cluster with a floor-area ratio (FAR) of 3 in a temperate climate, us-

ing a simulation-based, multi-objective algorithmic optimization method. In a previous study [47], design variants were manually generated from three base typologies—bar, tower, and courtyard—yielding regular shapes with a four-sided footprint. The present study expands the exploration to encompass a significantly larger pool of over 20,000 design variants. This broader scope includes buildings with irregular footprints, with the goal of discovering unconventional new solar species.

The method employed endeavors to enable the exploration of a wide design space, while overcoming several limitations associated to parametric modelling and multi-objective optimization (MOO), as highlighted in the previous section:

- Objectives: We adopt a balanced approach to multi-objective optimization by identifying two goal functions that well reflect the two primary strategies outlined by European energy legislation [72]: reducing the use of energy in buildings, while also increasing onsite energy generation potential. Focusing on just two performance targets enables us to visualize results on a two-dimensional graph, facilitating easy interpretation and visual exploration of emerging patterns and Pareto front solutions that optimize the objective functions simultaneously.
- Indicators: This study employs computationally friendly indicators as objective functions to streamline the optimization process. In temperate climates, and specifically for residential buildings, the effects of abundant annual radiation on the envelope (kWh/m^2) are generally positive for energy balance, as solar heating, daylighting, and renewable energy production are known to largely outweigh potential glare risk and overheating in the warm season. Compactness (S/V ratio) provides a second reliable yet easy-to-compute indicator as a proxy for detrimental heat gains and losses through the envelope.
- Design variables: The optimization process is based on geometric variables related to building massing, rather than considering factors such as fenestration layout or materials. This approach reflects a well-established sequence in design practice [73] and acknowledges a hierarchical relationship among decision variables [74]. Additionally, we employ a parametric modelling strategy, based on a number of cores and corridors, that generates only viable design variants, meeting structural and egress requirements. The research explores a "middle ground" of formal complexity, bridging the gap between the rectangular four-sided prisms that are typically mandated by urban planning regulations and the deeply articulated, voxelated, sculpted volumes of much contemporary architecture.

3.2. Workflow

The method presented here combines two alternative strategies traditionally employed in the performance evaluation of design variants—namely, a larger sample size versus higher simulation accuracy—into a two-step process.

Stage 1—Optimization process and correlation studies:

1. Stage 1 employs easy-to-compute indicators to explore a large pool of over 20,000 iterations, grouped in 20 sub-domains based on the number of vertical cores and horizontal connections. Design variants are generated by parametric modelling and optimized using a GA to reduce computing time, while also increasing the number of individuals and generations.
2. The results for each sub-domain are plotted on a two-dimensional graph for preliminary evaluation of emerging trends and correlations between geometric variables and energy indicators. Pareto front solutions are also documented through tri-dimensional illustrations and planimetric views of radiation and daylighting analysis, providing further insights into the optimization outcomes.

Stage 2—Detailed analysis and final ranking of Pareto front solutions:

3. Stage 2 evaluates 151 selected Pareto front solutions resulting from Stage 1, using full-climate analyses that are more accurate, but computationally expensive. Detailed graphs identify individual contributions for energy use (lighting, heating, cooling,

DHW) and energy production (from photovoltaic and solar thermal systems) for each variant, on both monthly and yearly bases.

4. The results are plotted on a bar graph based on total energy use, including positive and negative contributions, to determine a final ranking of the best performing solar species. Additionally, all 151 Pareto front cases are plotted on a graph illustrating energy demand versus energy production potential, also in relation to the Nearly Zero Energy Building (nZEB) target.

A scheme of the workflow is presented in Figure 1:

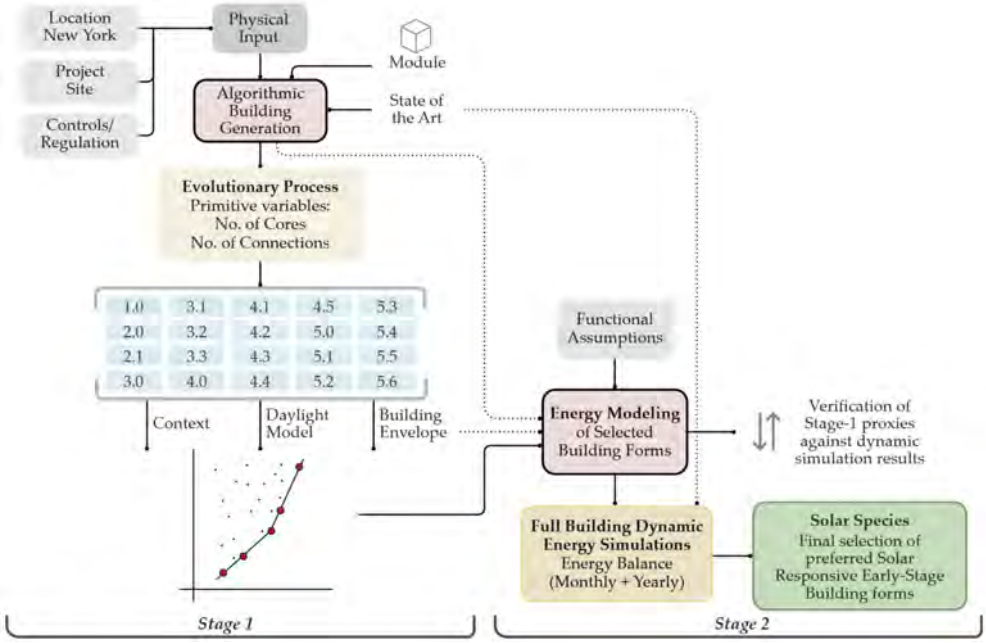

Figure 1. Scheme of the workflow.

3.3. Design Constants

The research primarily focuses on the formal and spatial attributes of buildings, distinct from materials, components, or systems. Consequently, all variables unrelated to building and urban form—such as the insulation values of walls and windows, climatic conditions, and heating and cooling systems—are held constant.

The simulated cases are situated within New York City, characterized by its mixed-humid climate classified as "Cfa" (cool and wet winters and hot and humid summers) according to the Köppen–Geiger climate classification system. The weather data are from 'La Guardia' station (New.York-LaGuardia.AP.725030: 40.779, −73.88) with Dry Bulb Temperature ranging between −10 and 35 °C, indicating a heating-dominated climate.

A building density of FAR 3 (floor-area ratio) is consistently applied across all design variants, aligning with the average density observed in urban residential areas of New York City. This value is also informed by previous studies, such as those by March and Trace [75], which identify a maximum FAR of 4 to ensure unobstructed daylighting penetration, and a minimum of approximately FAR 1.5 to maintain heat energy demand below 100 kWh/m^{2}y [76]. Moreover, compact urban forms resulting from a relatively high FAR offer additional ecological benefits, including reduced urbanized land use, transportation needs, and associated fuel consumption [77]. The building is simulated on a 100 × 100 m plot, surrounded by eight blocks separated by a 20 m wide street, with the same shape as the design iteration under evaluation. This arrangement is designed to account for the shading effect of the surrounding context (Figure 2).

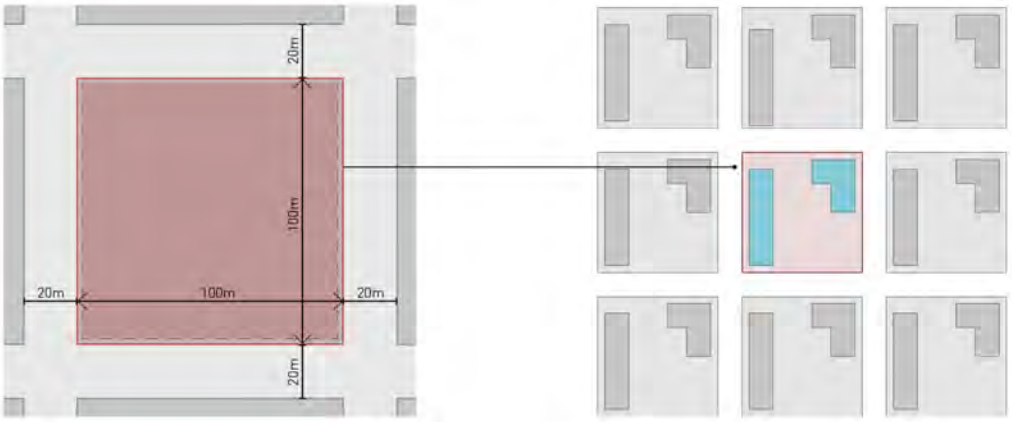

Figure 2. 100 × 100 m plot (**left**) and simulation setup (**right**).

3.4. Simulation Settings

Building performance analyses have been modeled using the climatic conditions of New York, defined by ASHRAE as Climate Zone 4A [78] and were conducted with Climate Studio, an environmental analysis plugin for Grasshopper [79].

Radiation and daylighting analyses are based on a progressive path-tracing version of the Radiance raytracer to calculate annual direct and indirect irradiation levels. The simulation uses sun and sky radiances from the local weather data file for New York City. The daylighting analysis grid was set at the work plane height of 0.76 m with a spacing of 1 m [80]. The grid spacing was chosen to strike a balance between simulation accuracy and computational efficiency, thereby optimizing simulation time. Building elements like ceiling, floor, and walls were segregated to assign relevant reflectance values. The glazing ratio was set at 0.3, a typical value for residential buildings, while thermal characteristics adhere to Energy Modelling Standards, based on recommendations outlined in ASHRAE 90.1-2004 [81] and tailored to climate zone, building program (residential), and surface type.

Energy demand simulations were conducted using EnergyPlus, with parameters modeled in accordance with the adaptive comfort normative (ISO 17772:2017) [82], utilizing a setpoint temperature of 20 °C for heating and 26 °C for cooling. The occupancy schedule reflects typical active usage period, and a separate artificial lighting schedule was deployed with a target illuminance level of 400 Lux throughout the regular occupied hours of 7:00 a.m. to 11:00 p.m. Energy-efficient LED fixtures (lighting power density of 7.5 W/m^2) with a dynamic dimming control have been used to ensure that the lighting load adapts to the natural light entering the occupied spaces. Material properties were defined according to a standard concrete construction assembly, with a U value of 0.2 W/m^{2}K for the external roofs and walls. The double-glazed windows have a solar heat gain coefficient of 0.33, visual light transmittance of 0.58, and a U-value of 1.44 W/m^{2}K.

Electricity requirements for heating and cooling are calculated by approximating the behavior of a realistic HVAC system with high-efficiency characteristics, defined as a heat pump operating for heating and cooling with a coefficient of performance COP = 3.

Domestic hot water demand is calculated based on the annual consumption for activities such as showering, hand washing, and laundry for the occupancy of one person every 30 m^2 and 48 L/person/day, following the method from Yao and Steemers [83]. It should be noted that solar thermal (ST) collectors are exclusively allocated to fulfil the demand for domestic hot water (DHW), thereby diminishing the required purchased energy for its production. Any DHW demand not met by solar thermal collectors is addressed by a heat pump, with the energy consumption converted into electricity using a value of COPDHW = 2.4, based on a high-performing product available on the market at the time of the research.

3.5. Parametric Form Generation

Our study takes an innovative approach to parametric form generation by acknowledging a fundamental requirement for means of egress in residential buildings, mandated by virtually every legislative framework worldwide, including The International Building Code [84] and the EN Eurocodes. This requirement entails vertical continuity of emergency stairs and limits the travel distance for the safe evacuation of building occupants. While structural necessities may still allow for inefficient or extravagant solutions—as much contemporary architecture clearly shows—safety requirements can be hardly evaded. Incidentally, these requirements often introduce a degree of rationality to both structure and internal layout, since egress stairs and elevator shafts, placed at regular intervals, usually double as load-bearing cores. Similarly, horizontal egress circulation confines residential units to three primary layouts: single- or double-loaded corridor and point load distribution (where stair cores reach every unit), with rare exceptions like a "skip-stop" solution found in some buildings with duplex apartments. Accordingly, our parametric modelling approach utilizes vertical cores and horizontal corridors as the base components to generate the layout of the floorplan and, consequently, the overall shape of the building (Figure 3).

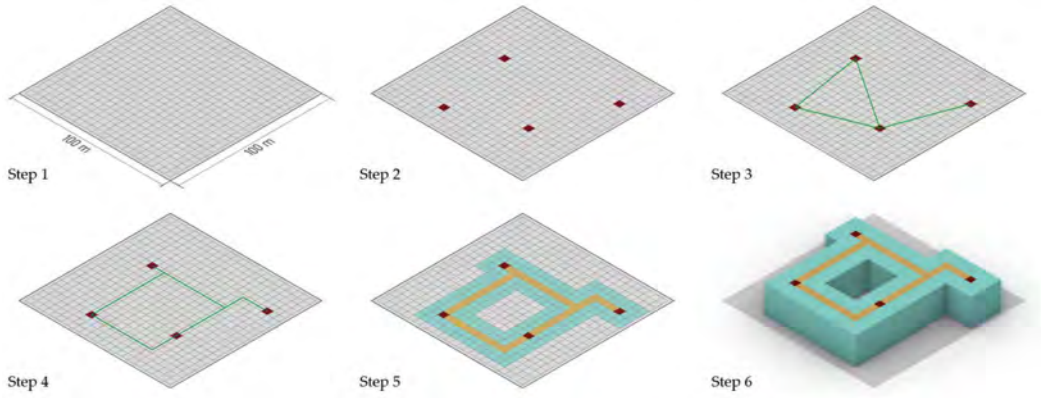

Figure 3. Parametric Modelling Steps.

The project site is subdivided into a 4 × 4 m grid (step 1), with each cell approximately the size of a typical vertical core in a mid-rise apartment building, for a total of 625 cells where a variable number of vertical cores can potentially be located by the algorithm (step 2) at a distance ranging between 20 m and 60 m. These cores are connected by a variable number of lines (step 3), which are then transformed into orthogonal corridors corresponding to the underlying grid (step 4), following a shortest-path logic. Residential units are subsequently added on each side of the corridors (double-loaded corridor) and around cores, with a depth of either one or two modules, resulting in a total floor depth of either 12 m or 20 m (step 5). Finally, the floor layout is extruded vertically to meet the maximum allowable built area of FAR 3, with all floors set at a height of 4 m (step 6).

Additional constraints have been imposed to narrow down the pool of variants to solutions with a better prospect of meeting the chosen objectives, ultimately reducing computational costs. The single-loaded corridor was excluded, as it is an inherently less compact circulation model compared to a double-loaded corridor; similarly, dead-end corridors were also excluded. Following the "passive zone" concept by Baker and Steemers [69], the depth of residential units is limited to two modules for a total of 8 m, or approximately twice the floor-to-ceiling height, so as to ensure sufficient daylighting over the entire floor area. For courtyard buildings, the study also sets a minimum distance between external walls to exclude solutions with a high probability of failing daylighting requirements. Volumetric continuity is guaranteed in all cases by extruding the building footprints to prevent excessive heat transfer and overshading associated with setbacks and cantilevers. Rather than generating extravagant yet unfeasible forms as seen in existing parametric design tools, the presented method ultimately produces a comprehensive set of design variants that would likely meet safety approval in most countries. The approach

retains all the advantages of using base typologies, such as structure and circulation coherence, without the drawbacks, such as precluding irregular layouts or unusual shapes.

3.6. Stage 1: Optimization Process and Correlation Studies

3.6.1. Performance Assessment

Stage 1 uses solar radiation intake as a reliable indicator for active energy potential and a key objective function for the optimization process:

- Total radiation (TR-400) is calculated as the total annual radiation falling over the envelope, both vertical and horizontal, on surfaces receiving annual mean radiation greater than 400 kWh/m^2. The metric is a well-established indicator for potential energy production by active solar systems (PVs).

At the same time, larger solar potential may result from arbitrarily increasing the envelope area of the building, at the expense of increasing total heat transfer and the related heating and cooling loads needed to maintain indoor comfort. Consequently, the study adopts building envelope area as an easy-to-compute geometric indicator of adverse heat gains and losses, serving as a second objective in the optimization process:

- Compactness (S/V ratio) is calculated as the ratio between envelope surface area and volume of the building; the metric is used as a proxy for heating and cooling energy demand, which tends to increase when a larger external envelope is used to enclose a given amount of volume.

Daylight factor (DF) is an easy-to-compute indicator for assessing visual comfort and the associated demand for electric lighting. A criterion of DF > 2% for the ground floor is utilized as a filtering measure, ensuring that only solutions meeting this threshold are considered. This requirement aligns with regulations and labels concerning energy efficiency, including those outlined in Italian legislation pertaining to Directive 2009/28/EC [85].

- Daylight Factor (%) is defined as the ratio between indoor illuminance at a point in the building and the outdoor horizontal illuminance under a CIE overcast sky.

3.6.2. Optimization Process

The optimization process by GAs employs the two main indicators (TR-400 and S/V ratio) as targets, through an iterative process based on the breeding of a 'successful' parent to converge towards improved solutions. In this case, the genetic code is the location of vertical cores from parent solutions. This process is facilitated by Octopus [86], a Grasshopper-based optimization tool utilizing the multi-objective evolutionary algorithm SPEA-2. Octopus generates trade-off solutions based on Pareto dominance [87], enabling the simultaneous optimization of all objectives. The two targets are diverging, given that active solar potential is inversely correlated with the envelope area. Consequently, the optimization process aims to identify trade-off solutions with minimal surface area intercepting maximum solar radiation.

Parametric modelling facilitates exhaustive exploration of the entire design space defined by the variables, while the selected geometry- and radiation-based indicators allow for swift computation (approximately 30 s per simulation) compared to full-climate simulations, resulting in the rapid sampling of over 20,000 design variants. The design space is divided into 20 sub-domains, each featuring a distinct number of cores and corridors, in part to alleviate the computational cost of the search, but also to analyze each group separately, so as to identify emerging patterns specific to each building sub-domain.

3.6.3. Evaluation of Results

Approximately 1000 viable solutions for each sub-domain are plotted on a matrix to facilitate the assessment of trends and correlations between energy indicators and geometric variables (Figure 4). Horizontal transects (e.g., line A in the figure) are extracted from the scatterplot to observe the evolution of building forms with identical S/V ratios, adapting to maximize solar availability. Additionally, detailed radiation and daylighting maps of up

to eight Pareto front solutions are presented using three-dimensional models in isometric view to showcase distribution patterns across each building cluster. The challenge lies in identifying qualitative formal traits that may not align with established typologies or morphology parameters. This study identifies specific geometric features, such as orientation, form factor, distance between buildings, and footprint articulation, which are most often associated with optimal solutions. These insights serve as tentative guidelines in the early-phase design of active energy buildings.

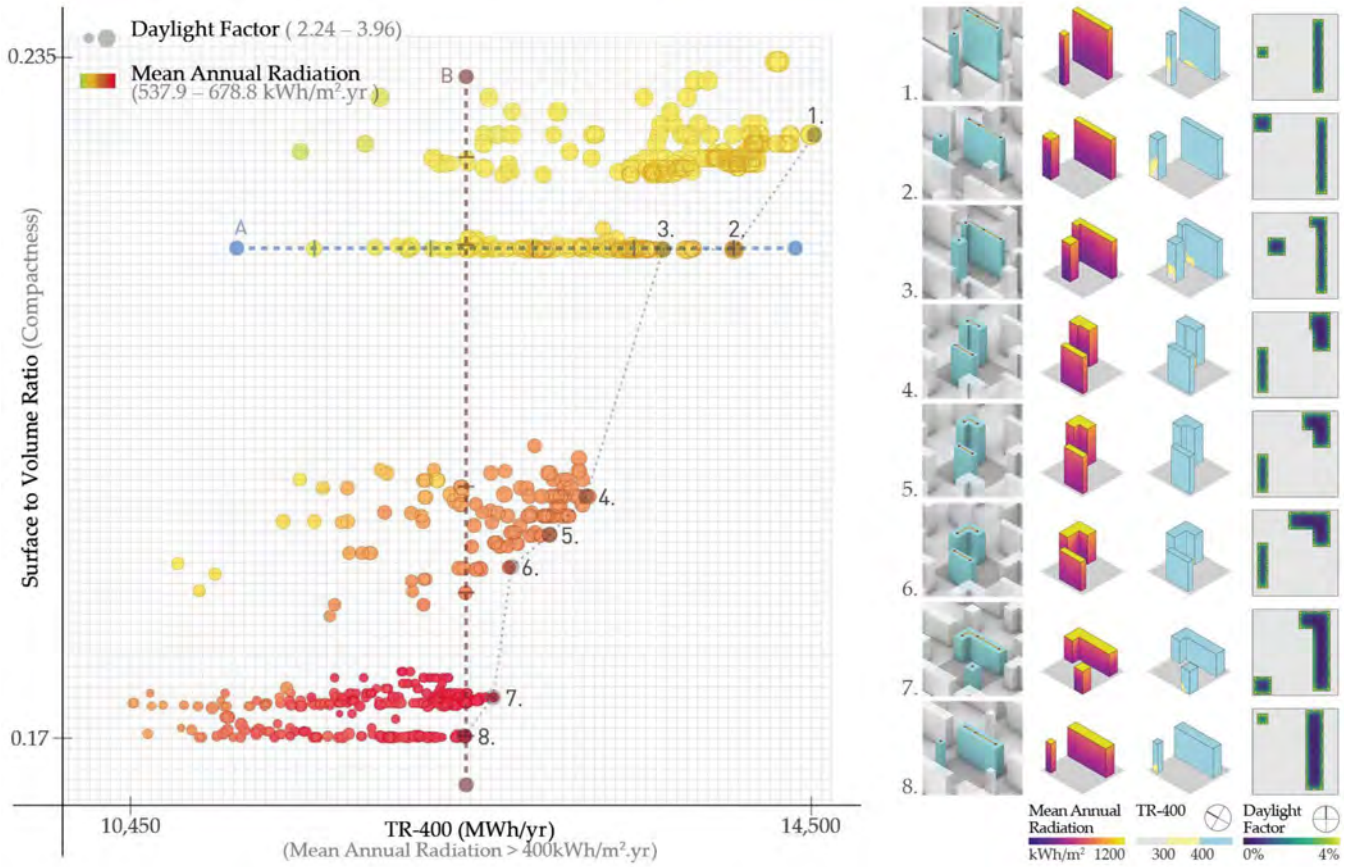

Figure 4. Example of first-stage output for sub-domain 4.2 (four vertical cores and two corridors).

3.7. Stage 2: Detailed Analysis and Final Ranking

3.7.1. Performance Assessment

Stage 2 evaluates and compares 151 Pareto front solutions resulting from Stage 1, using full-climate analysis to arrive to Annual Energy Production and Annual Energy Demand (Figure 5), defined as follows:

- Annual Energy Production (kWh/m^2) is determined by estimating the energy produced by photovoltaic (PV) panels and solar thermal (ST) collectors, using efficiency values of 0.2 and 0.7, respectively. These panels and collectors are mounted parallel to the surface of façades (vertical) and roofs (horizontal), based on the envelope area receiving an irradiation level from 300 to 400 kWh/m^2 for ST collectors and over 400 kWh/m^2 for PV panels. Among the eligible regions for PV, a coverage factor of 50% for roof and 80% for the opaque facade surfaces was applied.
- Annual Energy Demand (kWh/m^2) includes heating and cooling, appliances (4 W/m^2), domestic hot water (DHW), and artificial lighting based on case-specific daylighting conditions, calculated on an hourly basis. It was assumed that all these services would use electricity as a source, which would make the relative figures comparable. The energy for operating elevators was not included in the calculation.

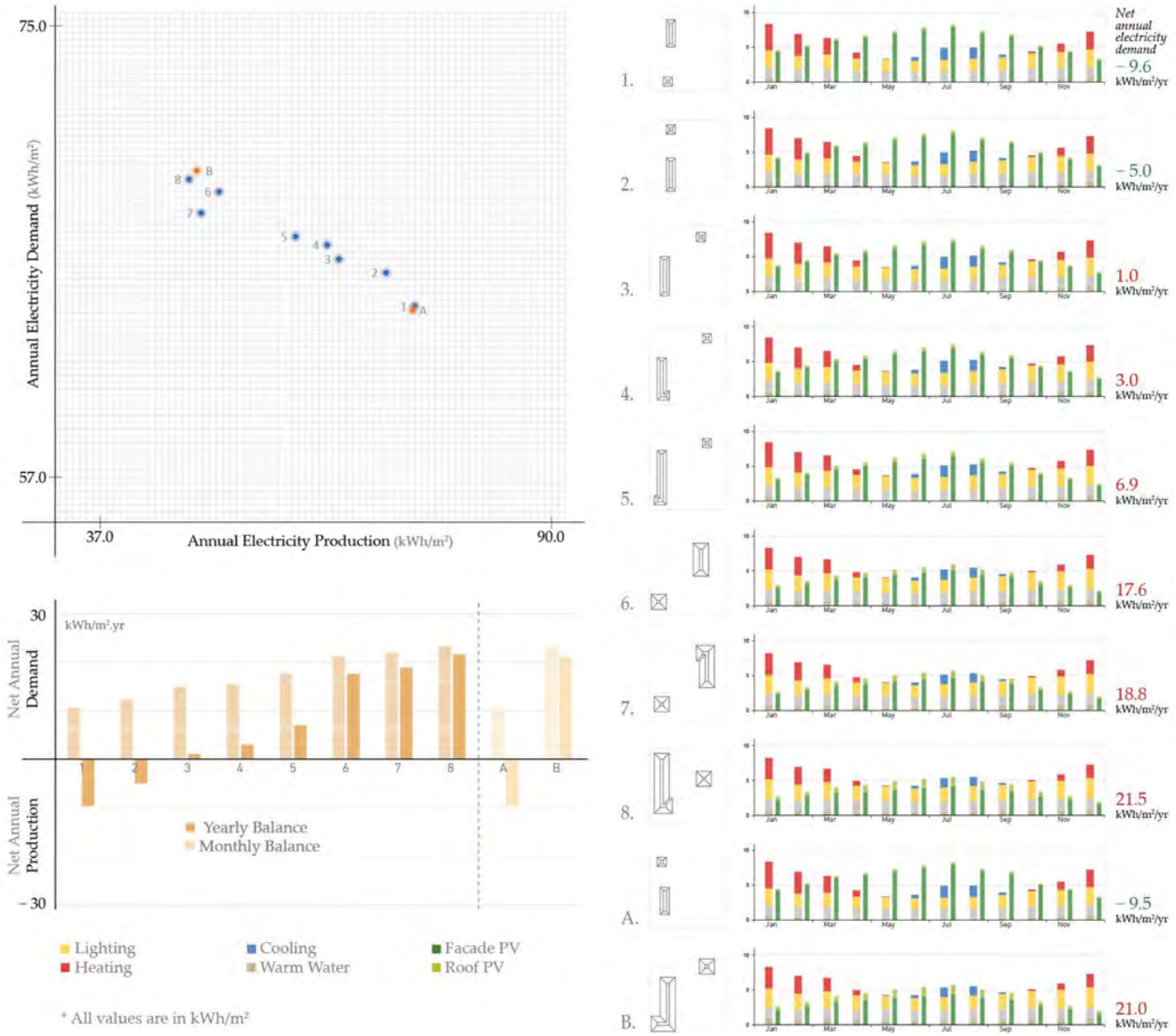

Figure 5. Example of second-stage output for sub-domain 3.1 (three vertical cores and one corridor). Cases 1 to 8 are Pareto front solutions, case A achieved highest mean daylight factor while case B received highest mean annual radiation during stage 1 evaluations.

3.7.2. Final Ranking

Finally, all Pareto front solutions are ranked on a bar graph based on Final Electricity Demand, including positive and negative contributions:

Final Electricity Demand (kWh) includes the electricity demand for heating and cooling, electric lighting and appliances, plus any electricity required to produce DHW not covered by ST collectors, minus the electricity produced by PV panels. It quantifies the energy purchased from the grid after accounting for the offset provided by onsite renewables. In addition to the comprehensive annual balance, a monthly balance analysis was also conducted. This analysis accounts for surplus electricity generated in one month separately from the demand in another month.

4. Findings

4.1. Stage 1: Optimization Process and Correlation Studies

In the initial stage, over 20,000 cases evaluated by the optimization algorithm are plotted on a graph (Figure 6) and assessed for their causal relationship between geometric variables and energy indicators. The scatterplot displays a well-established linear correlation between the two chosen indicators, as documented in the existing literature.

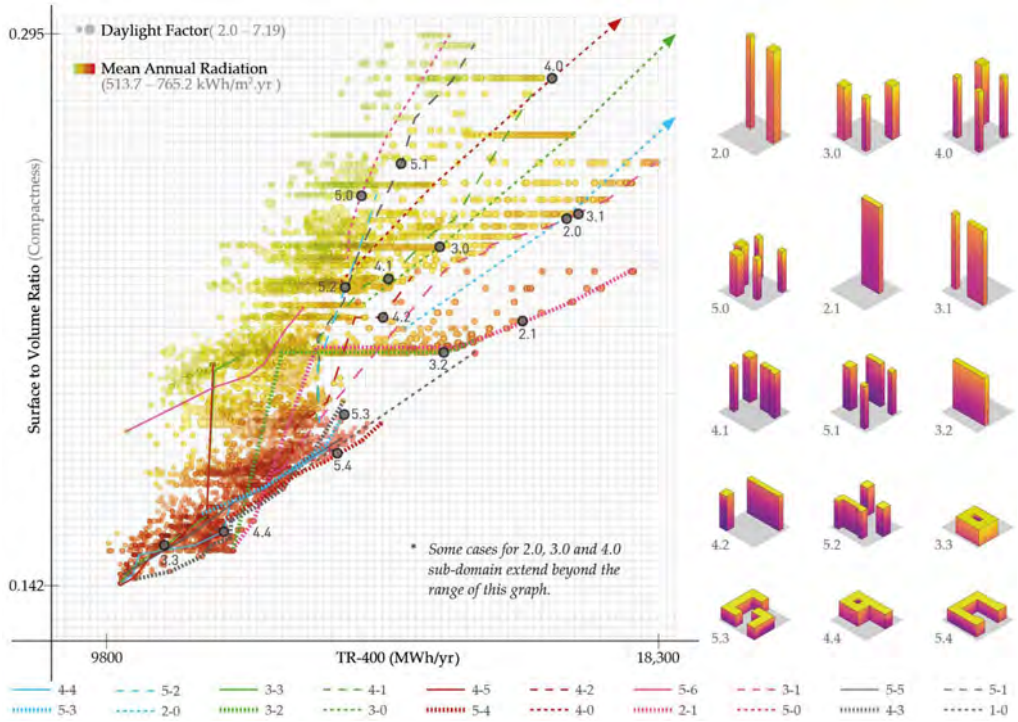

Figure 6. Stage 1 results from all sub-domains, with sample cases highlighted on the right.

It indicates that more compact buildings are typically linked to lower heating and cooling loads, but also associated to reduced radiation availability. Conversely, less compact buildings, generally taller and with a shallower footprint, may result in increased energy demand, but also display greater solar energy potential. This supposed equivalence in energy balance among Pareto front solutions with very different compactness (S/V ratio) is resolved through full-climate simulations conducted in the subsequent research phase. At the same time, the scatterplot underscores a significant degree of variability—up to a factor 1.8—in the amount of solar radiation falling on the envelope among solutions with an equivalent S/V ratio, as illustrated by the funnel shape of the plot. This means that solutions with comparable heat transfer and associated thermal loads can present very different levels of radiation exposure and potential energy production. The range in solar potential that cannot be fully captured by a single geometric indicator, hinges on precisely the kind of formal features that the paper attempts to uncover.

In this sense, horizontal transects extracted from scatterplots for each building subdomain provide valuable insights into the sequence of optimization steps taken by the GA, as related to variables such as distance between buildings, their aspect ratio, and orientation. In a way, transects offer a sectional view of the black-box evolutionary process, where each step of the sequence (left to right in Figures 7–15) unveils a gradual increase in solar radiation intake. As noted earlier, these transects intercept solutions with a constant S/V ratio, so that building geometry and layout are the only variables at play and formal traits associated with higher solar potential can emerge. Selected transects, illustrating clear optimization patterns resulting in higher active energy potential, are showcased below, arranged by the number of corridors connecting vertical cores.

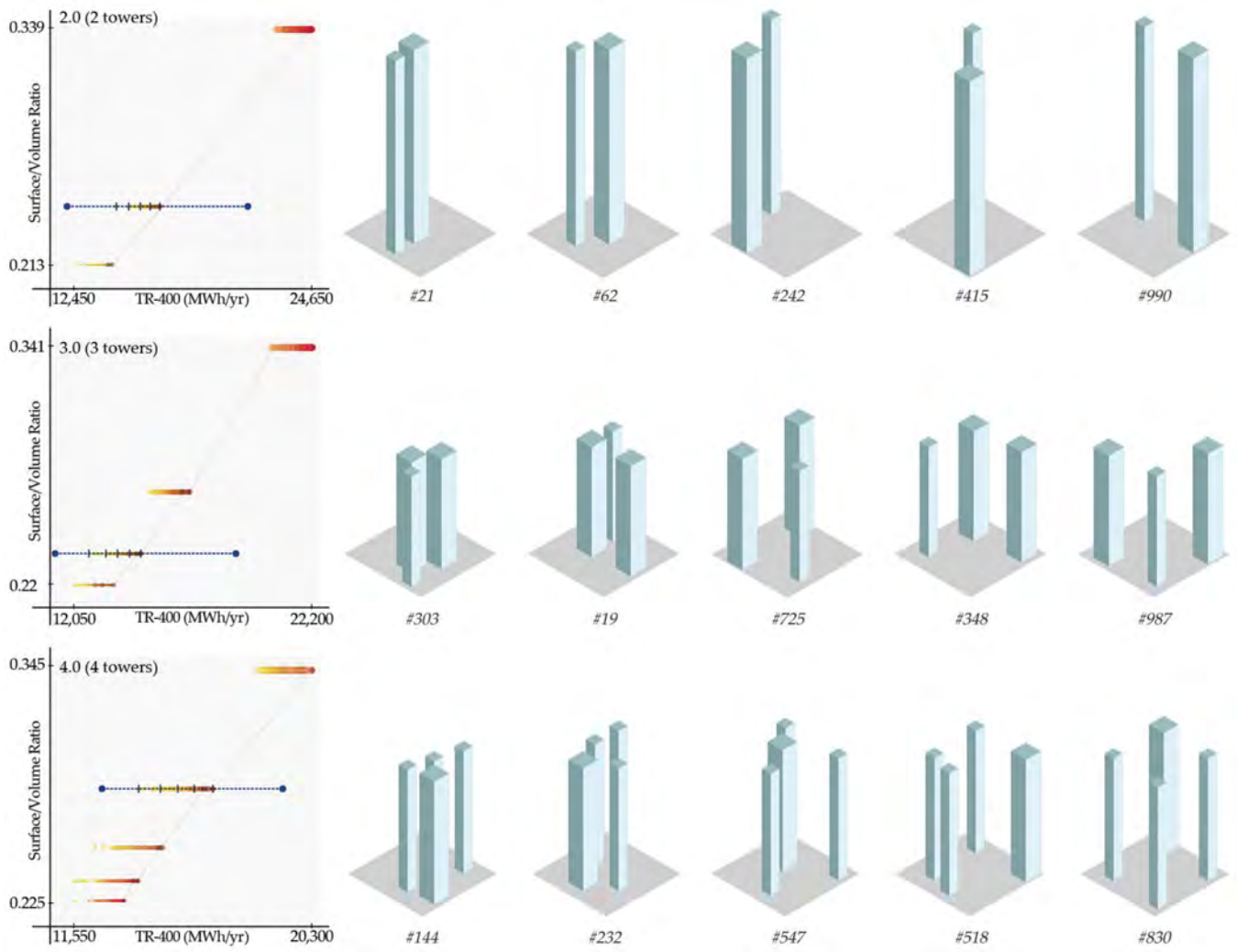

Figure 7. Transects for sub-domains 2.0, 3.0, and 4.0.

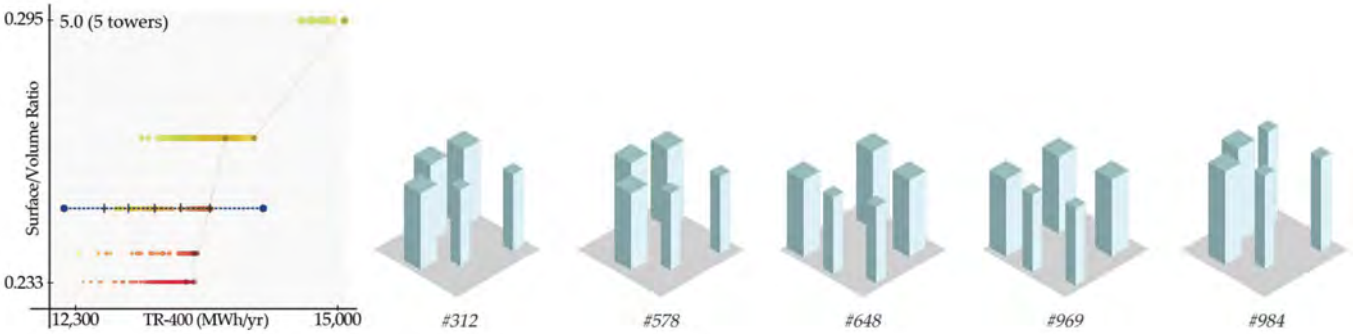

Figure 8. Transects for sub-domains 5.0.

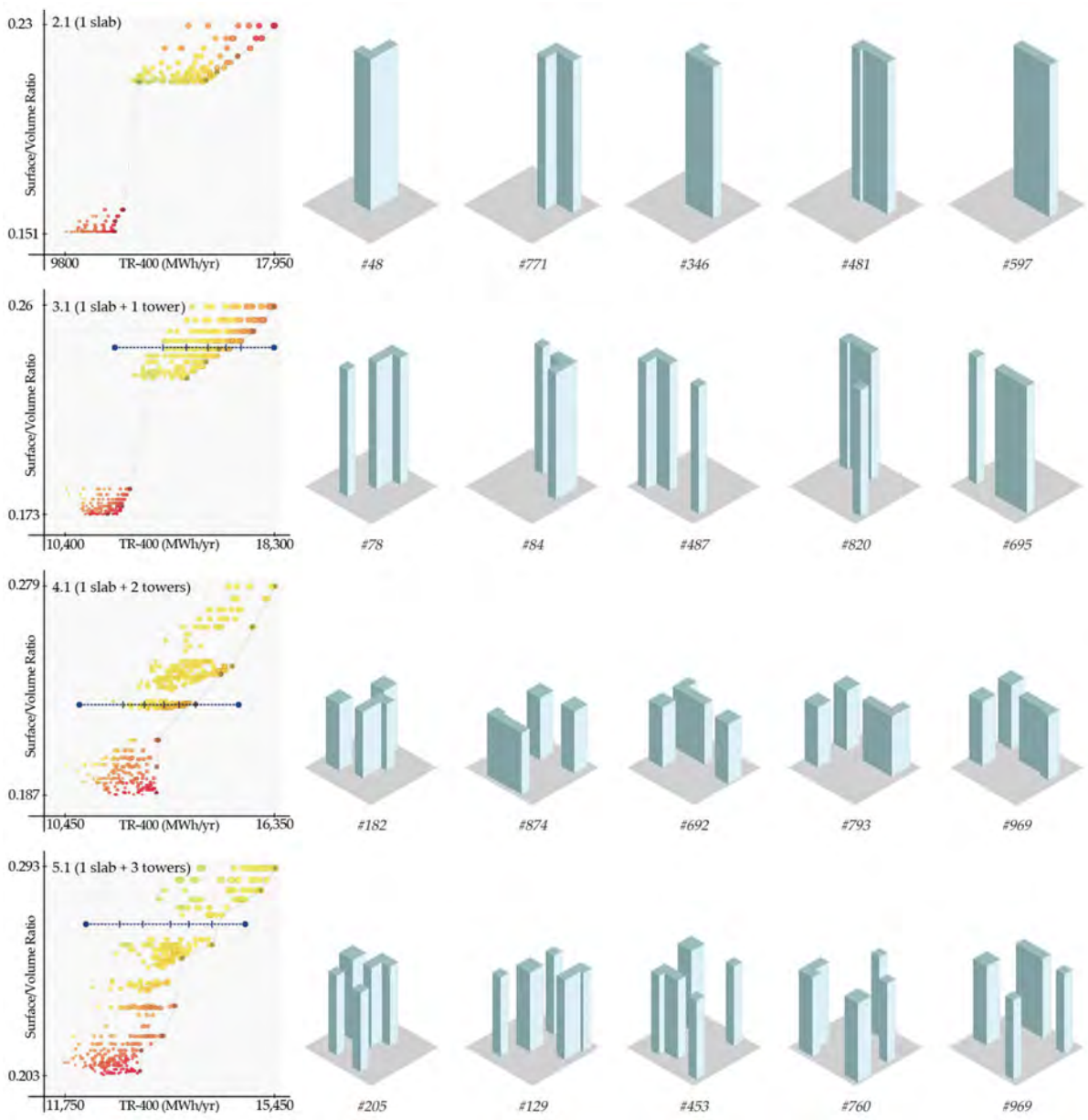

Figure 9. Transects for sub-domains 2.1, 3.1, 4.1, and 5.1.

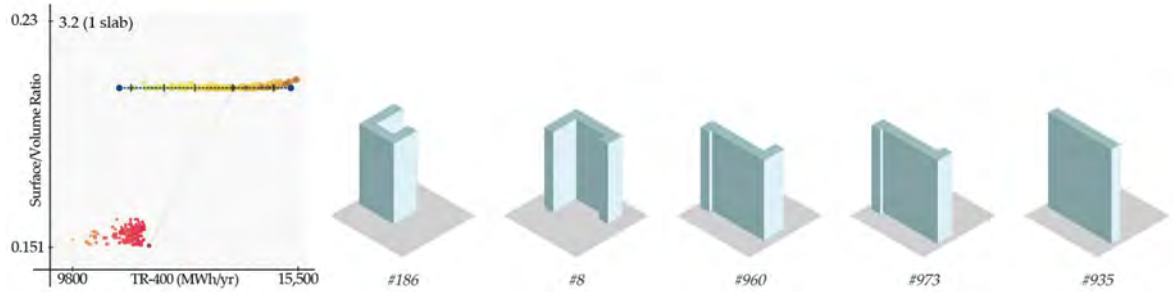

Figure 10. Transect for sub-domain 3.2.

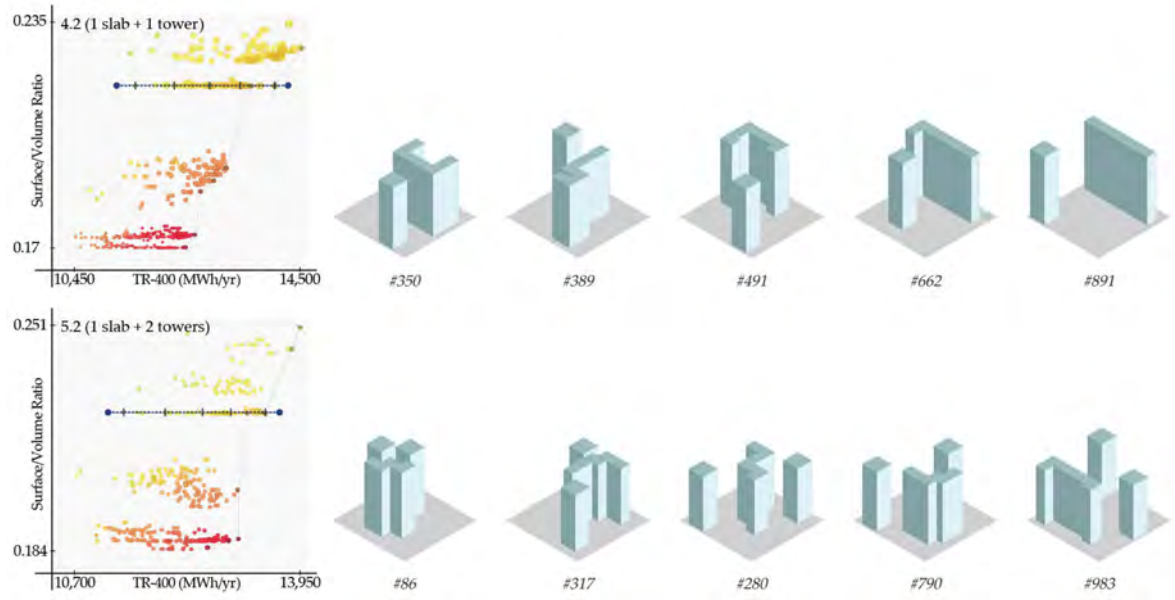

Figure 11. Transects for sub-domains 4.2 and 5.2.

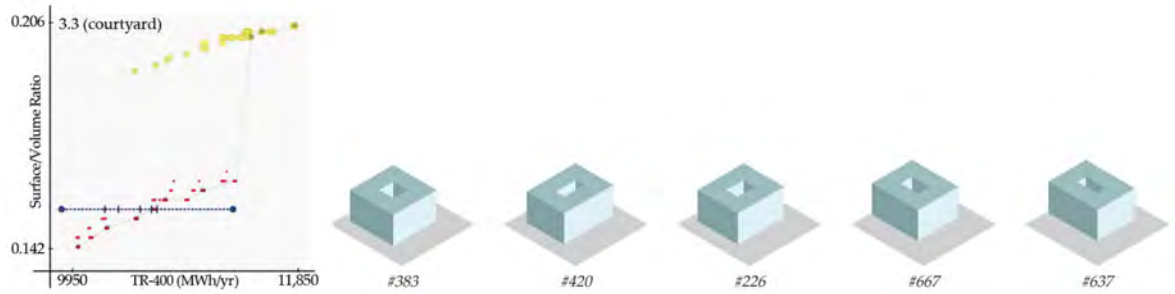

Figure 12. Transect for sub-domain 3.3.

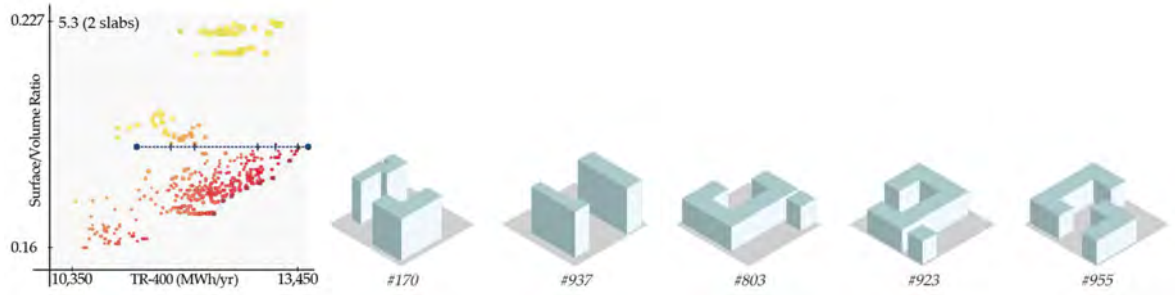

Figure 13. Transect for sub-domain 5.3.

Figure 14. Transect 4.4.

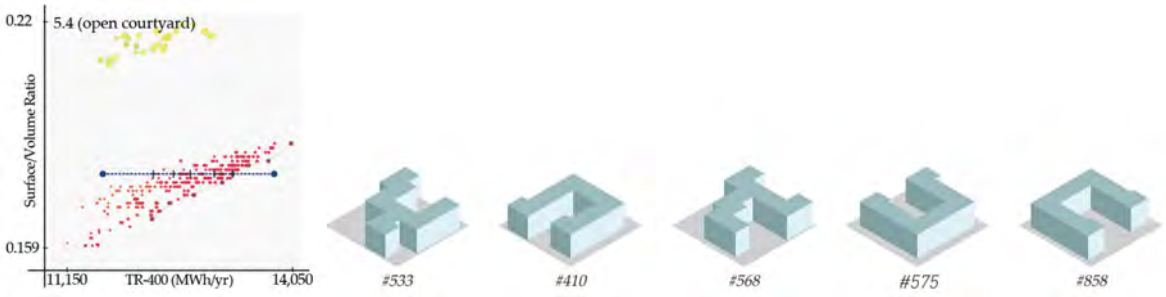

Figure 15. Transect 5.4.

4.1.1. Zero Corridors

One to four cores (Figure 7): Cases with no corridors and a variable number of cores result in clusters of skyscrapers exceeding 50 stories in height. Optimized layouts with one to four towers maintain a regular arrangement, with each tower occupying a corner of the plot. Three towers positioned diagonally (e.g., case #547 from Transect 4.0) emerge as an additional optimal layout in some cases. The optimization sequence shows a clear trend: towers positioned farthest from each other experience reduced overshadowing, thereby maximizing solar intake. For the same reason, setbacks from the plot's edge ensure that the closest distance between towers within the plot equals the closest distance between towers on adjacent plots.

Five cores (Figure 8): Five towers on the plot reveal a different pattern from cases with fewer towers, with no preferred configuration or evident trend. Optimization sequence shows that towers move away from each other, but do not settle into any stable arrangement, aside from a vaguely circular layout. Notably, four cores per hectare mark a clear threshold between grid-like alignment and more dynamic configurations.

4.1.2. One Corridor

One to five cores (Figure 9): Various combinations of one slab and up to three towers show similar trends as observed in groups of towers: buildings separate from each other and settle along the perimeter, with slabs invariably oriented along the north–south axis.

4.1.3. Two Corridors

Three cores (Figure 10): Two corridors produce volumes with a pronounced horizontal development that highlight a remarkable trend: out of approximately 1000 configurations with intricate footprints, Pareto front solutions consistently manifest as straight bars oriented in a north–south direction. This observation suggests that the linear volumes often favored by modernist architects would prove beneficial from an energy standpoint as well, but only if integrated by active energy systems, a technology that did not exist at the time.

Four to five cores (Figure 11): Additional elevators result in clusters with one to two towers competing with the slab for solar exposure. As already observed in cases involving multiple towers, optimal configurations for these clusters exhibit similar traits: buildings occupy the edges of the plot, with straight slabs oriented in a north–south direction.

4.1.4. Three Corridors

Three cores (Figure 12): The optimization process for compact courtyards is driven by at least two competing pressures: the first sets back the boundary of the building from the plot perimeter to mitigate overshadowing from neighboring structures. Conversely, the second one tends to widen the interior courtyard to increase solar exposure on the internal facades. The result is a courtyard elongated along the north–south axis.

Five cores (Figure 13): In line with configurations with five towers, this sub-domain produces flexible layouts with two L- or U-shaped bar buildings facing each other, positioned at the maximum distance allowed by the lot. These solutions are all comparable in terms of solar radiation intake, while offering a diverse range of configurations at the ground level that holds promise in characterizing open spaces within the plot.

4.1.5. Four Corridors

Four cores (Figure 14): Transect 4.4 reaffirms a prevailing trend toward regular-shaped courtyard buildings, while also introducing a potentially novel hybrid species: courtyards featuring a wing extension towards south.

Five cores (Figure 15): Transect 5.4 explores a wide range of irregular low-rise building configurations, but invariably produces Pareto front solutions that are wide courtyards open to the south. Once again, the recurrent trend toward regular footprints with minimal articulation is in full display.

4.2. Stage 2: Detailed Analysis and Final Ranking

In Stage 2, 151 Pareto front solutions obtained from Stage 1 are evaluated and compared, using full-climate analysis to establish a ranking based on net electricity demand (Figure 16), including positive and negative contributions to the energy balance. Vertical development characterized by any number of cores and fewer corridors notably produces a substantial majority of the top-performing cases. Conversely, horizontal development, resulting from two or more corridors, consistently exhibits lower performances. The first 35 cases in the ranking have one or no corridors, while the first building with more than two corridors (54.1), a courtyard open toward the south, appears in position 68; spanning just six floors, this is also the highest-ranking mid-rise building. A parallel trend emerges with slenderness: slim volumes with a single 4 m module on each side of the corridor (12 m total thickness) consistently outperform buildings with a deeper footprint. While a few thicker towers appear in well-performing configurations, the first slab building with an 8 m module on each side (20 m total thickness) ranks at position 62 (41.6).

Three broad groups of buildings emerge from the final ranking, identified by a color gradient band, underscoring the significance of vertical development and slenderness in optimizing urban form:

- Group 1—Skyscrapers (over 40 stories): A first subset of approximately 20 clusters, including one to four exceptionally tall and slender buildings, mostly without corridors, contributes the bulk of positive and nearly zero energy solutions. Final electricity demand: below 0 kWh/m^2/year.
- Group 2—High-rises (15 to 40 stories): The subsequent section comprises approximately 60 clusters with three to five towers and slabs arranged in diverse configurations, with a gradually deeper footprint and only one or two corridors. Final electricity demand: between 0 and 10 kWh/m^2/year.
- Group 3—Mid-rises (6 to 15 stories): The final group encompasses roughly 70 clusters of distinctly lower buildings showcasing accentuated horizontal development and three to six corridors each. Final electricity demand: between 10 and 35 kWh/m^2/year.

These findings confirm the validity of the chosen indicators from phase 1, while also highlighting the outsized role that radiation intake plays in determining the overall outcome, as vividly illustrated by comparing positive and negative energy contributions for each optimized solution (Figure 17).

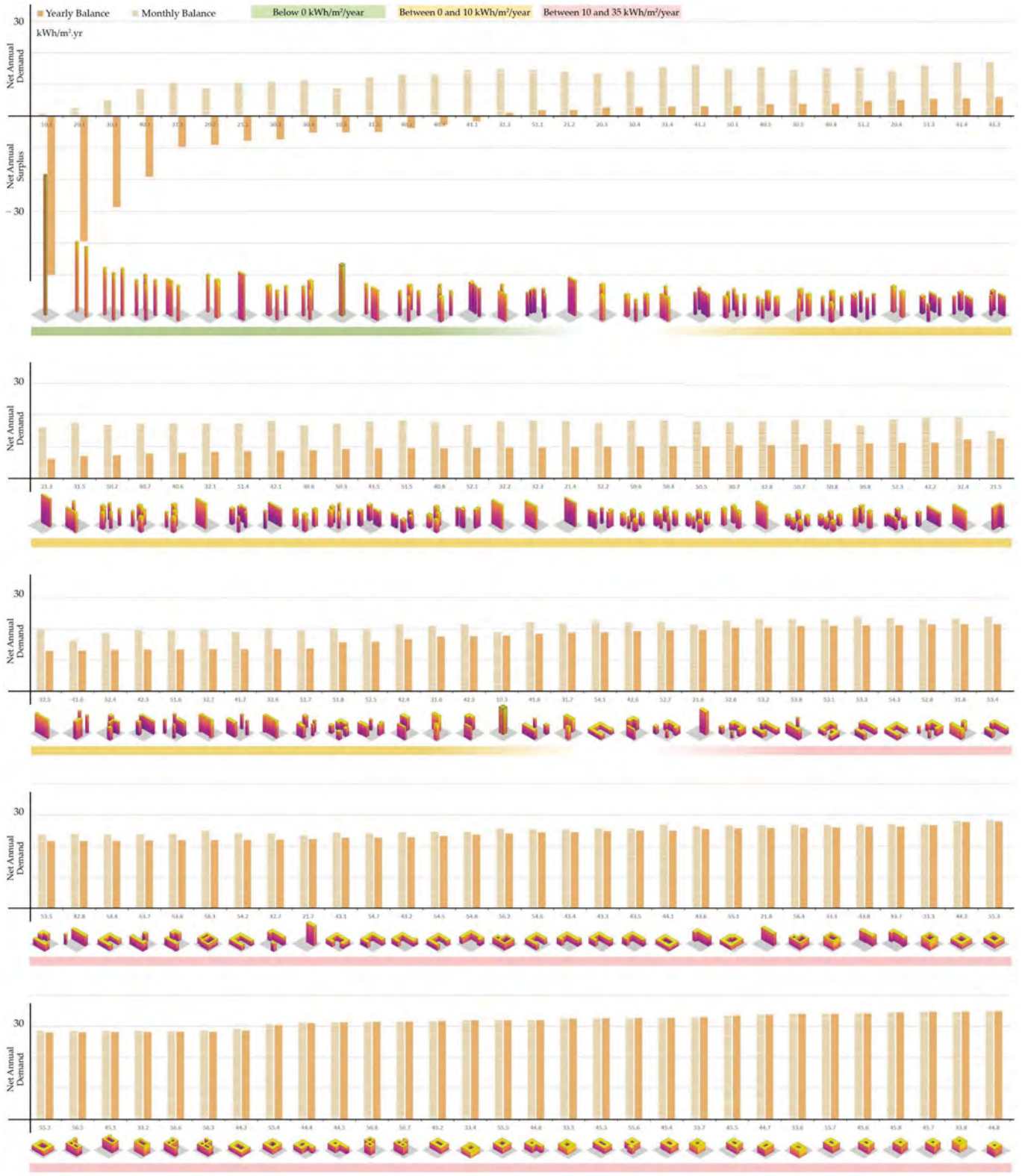

Figure 16. Final ranking of 151 Pareto front solutions based on final electricity demand.

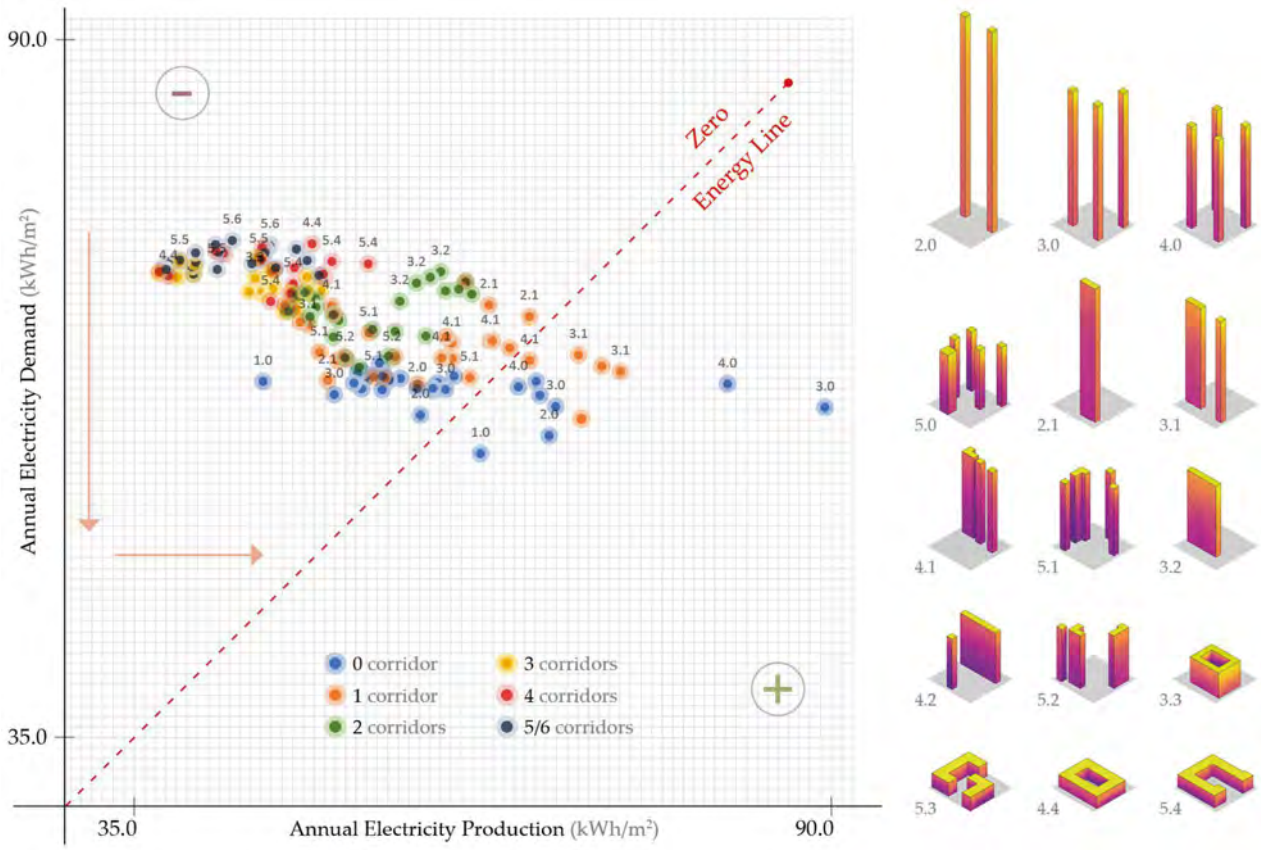

Figure 17. Positive and negative energy contributions for each optimized solution. The vertical axis represents the total annual electricity demand, while the horizontal axis represents the total annual electricity production from PV panels.

The 45° slope indicates cases for which, over the course of a year, electricity generated from PV panels matches the demand. Cases falling to the right of this line indicate instances where electricity production exceeds demand. It is intriguing to note that while the annual electricity demand fluctuates within a relatively narrow range across these cases, spanning from 57 to 75 kWh/m^2/year, the range of active solar potential significantly widens, ranging from 37 to 110 kWh/m^2/year, once the annual electricity production is accurately calculated. It can be inferred that the impact of building shape on annual electricity demand diminishes once artificial lighting is factored in the energy balance. Buildings that are less compact use less artificial lighting, mitigating the effects of higher heating and cooling loads typically associated to greater envelope area, while still producing a larger amount of electricity. What initially appeared as a conflict between competing objectives—low energy use versus high onsite energy fraction—requiring trade-off solutions, turns into a clear dominance of active solar potential in Phase 2.

5. Discussion

At the conclusion of Phase 1, the optimization outcomes reveal consistent trends across a diverse range of typologies toward regular shapes with minimal footprint articulation, maximum distance between buildings, a prevalent orientation along the north–south axis, and an open front facing towards the south. These discernible traits offer architects and urban planners a tentative set of guidelines for designing active energy buildings in the early stages of the design process (Figure 18). The results show the importance of reducing overshading caused by articulated footprints and tightly packed buildings that exacerbate heating and cooling demand, with only a marginal improvement in useful daylighting or radiation on the envelope.

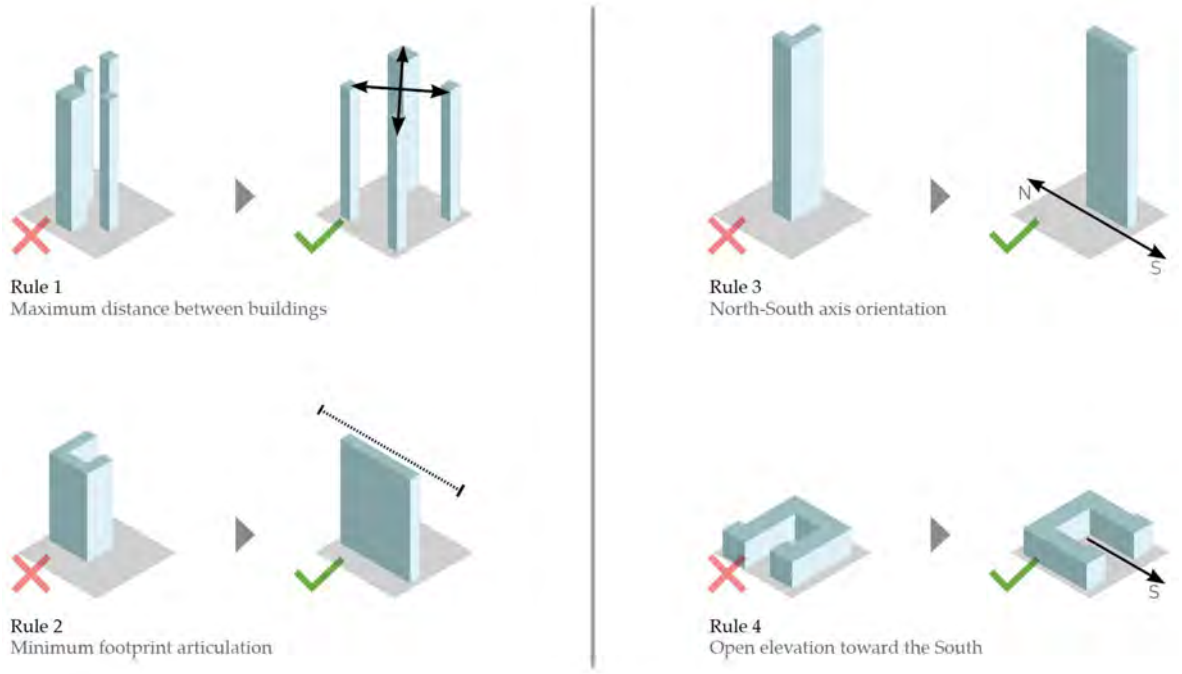

Figure 18. Set of guidelines for designing active energy buildings in the early stages of the design process.

Furthermore, the study suggests that vertical cores and horizontal connections may offer a novel and effective approach to characterize urban morphology in relation to onsite energy fraction and nZEB potential. Taller buildings with fewer corridors consistently outperform lower horizontal buildings, offering higher on-site energy potential without increasing energy demand. If we were to extrapolate these outcomes as planning guidelines, for example, configurations with up to four vertical cores (without horizontal connections) per hectare would yield a regular grid of very tall towers with significant solar potential and a positive energy balance. Conversely, the addition of one more core would lead to a markedly different outcome, resulting in an irregular layout and increased energy demand.

The research shows that these guidelines facilitate an increase in active solar potential and subsequent energy production, without increasing envelope area, thereby maintaining energy demand at a relatively constant level. While the current focus of the research centers on operational energy, it is evident that minimizing envelope area would yield higher embodied energy and carbon emissions as well.

At the same time, the shapes optimized by these routines in Phase 1 yield a broad range of energy performance outcomes by the conclusion of Phase 2. Once all energy inputs are calculated, including heating and cooling, artificial lighting, equipment, and domestic hot water, a clear hierarchy emerges among sub-domains. These results indicate that each sub-domain correlates with a specific range of solar potential, suggesting that the number of vertical and horizontal connections could serve as an effective new metric for characterizing urban form in terms of energy potential.

The "genetic code" of cores and corridors, subjected to environmental pressures aimed at maximizing solar exposure while minimizing energy consumption, generates veritable solar species with recognizable traits, in terms of number and orientation, shape, and layout of buildings on the plot (Figure 19). Crucially, these species exhibit a unique 'metabolic' rate of energy use resulting from their specific formal traits. Collectively, these findings suggest the descriptive and predictive power of solar species as a promising heuristic model for characterizing urban form in relation to both passive and active solar potential.

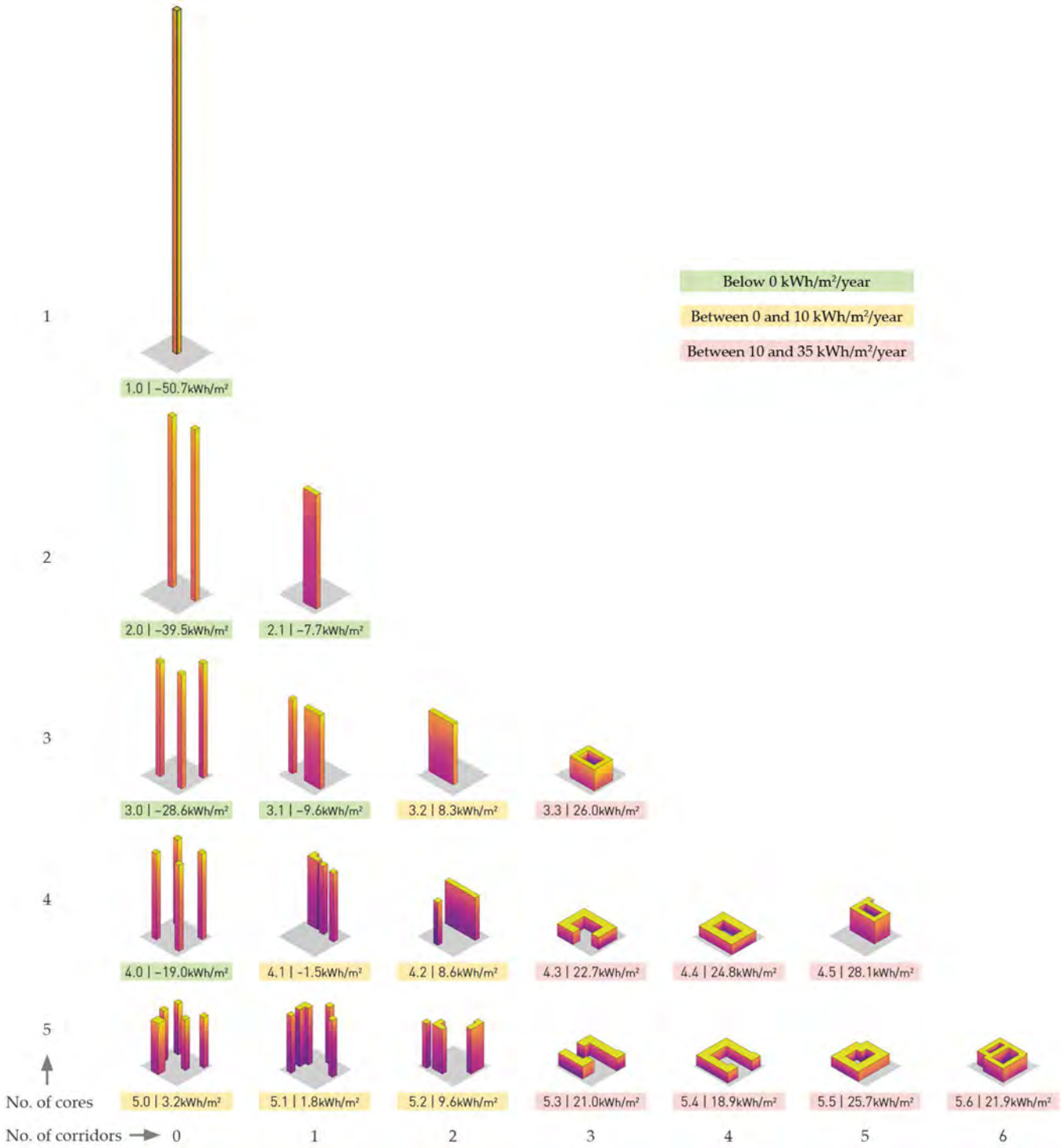

Figure 19. Taxonomy of Urban Solar Species.

6. Conclusions

The results of this research show that active solar potential should be a first-order priority in the design of energy-efficient buildings, particularly when solely operational energy is taken into account, as the variation in the potential for electricity generation is approximately three times as large as any concurrent variation in energy demand, due to shape alone. Rapid progress in BIPV and HVAC technology, as well as the use of additional methods of on-site energy harvesting not considered in this study, would of course result in different outcomes. Consequently, a larger number of massing configurations may result in scenarios where the

onsite energy production matches or even surpasses the annual energy requirement. It should be noted that these results were obtained under the assumption of a well-insulated envelope. Future research should explore the implications of incorporating embodied energy and carbon emissions related to building structure and envelope into the calculations.

The nearly-zero energy urban model that emerges from these analyses points to a predominantly vertical city, reminiscent of the recent proliferation of super-tall buildings in metropolitan centers worldwide. Moreover, this research offers a range of low-energy formal solutions for groups of more conventional high rises and for mid-rises with an articulated footprint. These solutions can be tailored to support pedestrian traffic, accommodate a mixed-use ground floor, meet building height restrictions, and maintain street-wall continuity.

Perhaps the most notable revelation of the study, however, is that given the opportunity to manifest in any of 20,000 different configurations, virtually all the best-performing buildings are utterly regular and somewhat aligned with conventional wisdom. In fact, these high-performing champions bear a striking resemblance to ordinary buildings found in our cities.

This circumstance suggests that today's architects and city planners may not be too far removed from realizing a sustainable future in construction—and that common sense could ultimately prevail in addressing our energy crisis. Interestingly, the results also testify to the ability of a purely automated process to produce outcomes that closely mimic human design logic. However, this apparent simplicity and familiarity of solar species can be deceptive. While their traits may seem reassuringly familiar, they adhere to a set of subtle rules that can be easily overlooked. It is the rigorous application of these elementary yet specific guidelines that ultimately determines their success.

Another lesson is abundantly clear—and not as subtle: much extravagant architecture today appears to suggest that geometric complexity may be the key to efficient buildings. This study concludes that extreme sobriety of form can also lead to significant energy efficiency gains.

On the other hand, the broad formal diversity observed among optimized solutions with comparable energy performance also challenges a common misconception that automated design methods are overly deterministic and tend to produce too narrow a range of solutions. Just as nature offers millions of different organic species as solutions to the same problem of survival and reproduction, the genetic algorithm-based search presented in this study yields hundreds of formal solutions with comparable performance to the same challenge of achieving energy efficiency. Within this range of optimal shapes, other key parameters such as program, spatial quality, or aesthetic preference of architect and client should naturally play a central role in determining the final outcome.

Architectural design has often been perceived as a process of trade-offs, where improvements in one aspect—such as natural daylight or ventilation by increasing envelop area—can only be achieved at the expense of others, like detrimental heat transfers or glare risk. Indeed, conflicting objectives serve as the primary mechanism for generating variation in design, akin to the range of competing demands driving natural selection and evolution in organisms. As a result, multi-objective optimization is likely to remain a fundamental strategy in the design of buildings. On the other hand, the utilization of automated design methods, soon to include the deployment of neural networks, will continue to address these conflicting targets, streamlining the search for enhanced building forms. As part of this quest, the present study resolves a trade-off between active and passive energy potential in favor of solutions that excel in achieving both targets, at least until technology innovation will bring new parameters to bear on the form of buildings, thereby expanding, once again, the search for optimal solar species.

Author Contributions: Conceptualization: S.G., A.K. and G.M.; data curation: A.K.; investigation: S.G. and A.K.; methodology: S.G., A.K. and G.M.; software: A.K.; supervision: S.G. and G.M.; visualization: A.K.; writing—original draft: S.G. and A.K.; writing—review and editing: S.G. and G.M. All authors have read and agreed to the published version of the manuscript.

Funding: This research received no external funding.

Institutional Review Board Statement: Not applicable.

Informed Consent Statement: Not applicable.

Data Availability Statement: Further data can be shared upon request.

Conflicts of Interest: The authors declare no conflicts of interest.

References

1. Neufert, E. *Bauentwurfslehre*, 1st ed.; Bauwelt: Berlin, Germany, 1936.
2. Smil, V. *Energy and Civilization: A History*; THE MIT Press: Cambridge, MA, USA, 2017.
3. IEA; UNEP. *2019 Global Status Report for Buildings and Construction*; International Energy Agency: Paris, France; United Nations Environment Programme: Nairobi, Kenya, 2019.
4. IEA. *Energy Policies of IEA Countries: France 2016*; International Energy Agency: Paris, France, 2016.
5. Pérez-Lombard, L.; Ortiz, J.; Pout, C. A review on buildings energy consumption information. *Energy Build.* **2008**, *40*, 394–398. [CrossRef]
6. IEA. *Net Zero Roadmap: A Global Pathway to Keep the 1.5 °C Goal in Reach*; International Energy Agency: Paris, France, 2023.
7. Regulation (EU) 2021/1119 of the European Parliament and of the Council of 30 June 2021 Establishing the Framework for Achieving Climate Neutrality and Amending Regulations (EC) No 401/2009 and (EU) 2018/1999 ('European Climate Law'). 9 7 2021. Available online: http://data.europa.eu/eli/reg/2021/1119/oj (accessed on 12 February 2022).
8. Williams, J.; Mitchell, R.; Raicic, V.; Vellei, M.; Mustard, G.; Wismayer, A.; Yin, X.; Davey, S.; Shakil, M.; Yang, Y.; et al. Less is more: A review of low energy standards and the urgent need for an international universal zero energy standard. *J. Build. Eng.* **2016**, *6*, 65–74. [CrossRef]
9. Belussi, L.; Barozzi, B.; Bellazzi, A.; Danza, L.; Devitofrancesco, A.; Fanciulli, C.; Ghellere, M.; Guazzi, G.; Meroni, I.; Salamone, F.; et al. A review of performance of zero energy buildings and energy efficiency solutions. *J. Build. Eng.* **2019**, *25*, 100772. [CrossRef]
10. Tian, Z.; Zhang, X.; Jin, X.; Zhou, X.; Si, B.; Shi, X. Towards adoption of building energy simulation and optimization for passive building design: A survey and a review. *Energy Build.* **2018**, *158*, 1306–1316. [CrossRef]
11. Verdonck, E.; Weytjens, L.; Verbeeck, G.; Froyen, H. Design support tools in practice. The Architects' Perspective. In Proceedings of the 14th International Conference on Computer-Aided Architectural Design, Liege, Belgium, 7–10 November 2011.
12. Schlueter, A.; Geyer, P. Linking BIM and design of experiments to balance architectural and technical design factors for energy performance. *Autom. Constr.* **2018**, *86*, 33–43. [CrossRef]
13. Attia, S.; Gratia, E.; Herde, A.D.; Hensen, J.L. Simulation-based decision support tool for early stages of zero-energy building design. *Energy Build.* **2012**, *49*, 2–15. [CrossRef]
14. Weiler, V.; Harter, H.; Eicker, U. Life cycle assessment of buildings and city quarters comparing demolition and reconstruction with refurbishment. *Energy Build.* **2017**, *134*, 319–328. [CrossRef]
15. United Nations Environment Programme. *Global Status Report for Buildings and Construction—Beyond foundations: Mainstreaming Sustainable Solutions to Cut Emissions from the Buildings Sector*; United Nations Environment Programme: Nairobi, Kenya, 2024.
16. Heiselberg, P.; Brohus, H.; Hesselholt, A.; Rasmussen, H.; Seinre, E.; Thomas, S. Application of sensitivity analysis in design of sustainable buildings. *Renew. Energy* **2009**, *34*, 2030–2036. [CrossRef]
17. Dylewski, R.; Adamczyk, J. Economic and environmental benefits of thermal insulation of building external walls. *Build. Environ.* **2011**, *46*, 2615–2623. [CrossRef]
18. Hopkinson, R.G.; Petherbridge, P.; Longmore, J. *Daylighting*; Heinemann: London, UK, 1966.
19. Kheiri, F. Optimization of building fenestration and shading for climate-based daylight performance using the coupled genetic algorithm and simulated annealing optimization methods. *Indoor Built Environ.* **2019**, *30*, 195–214. [CrossRef]
20. Whillier, A. Solar Energy Collection and Its Utilization for House Heating. Ph.D. Thesis, Department of Mechanical Engineering, Massachusetts Institute of Technology, Cambridge, MA, USA, 1953.
21. Harish, V.; Kumar, A. A review on modeling and simulation of building energy systems. *Renew. Sustain. Energy Rev.* **2016**, *56*, 1272–1292. [CrossRef]
22. The American Institute of Architects. *2030 By the Numbers: The 2019 Summary of the AIA 2030 Commitment*; The American Institute of Architects: Washington, DC, USA, 2020.
23. Nguyen, A.-T.; Reiter, S.; Rigo, P. A review on simulation-based optimization methods applied to building performance analysis. *Appl. Energy* **2014**, *113*, 1043–1058. [CrossRef]
24. The Building Energy Software Tools Directory. Available online: https://www.ibpsa.us/best-directory-list/ (accessed on 10 November 2023).
25. Gagne, J.M.; Andersen, M.; Norford, L.K. An interactive expert system for daylighting design exploration. *Build. Environ.* **2011**, *46*, 2351–2364. [CrossRef]
26. Sola, A.; Corchero, C.; Salom, J.; Sanmarti, M. Multi-domain urban-scale energy modelling tools: A review. *Sustain. Cities Soc.* **2020**, *54*, 101872. [CrossRef]
27. Berge, A.; Johansson, P. *Literature Review of High Performance Thermal Insulation*; Chalmers University of Tech: Gothenburg, Sweden, 2012.

28. Giostra, S.; Masera, G.; Pesenti, M.; Pavesi, P. Use of 3D tessellation in curtain wall facades to improve visual comfort and energy production in buildings. In *IOP Conference Series: Earth and Environmental Science, Proceedings of the SBE19—Resilient Built Environment for Sustainable Mediterranean Countries, 4–5 September 2019, Milan, Italy*; IOP: Pune, Maharashtra, 2019.
29. Hamdy, M.; Hasan, A.; Siren, K. Applying a multi-objective optimization approach for Design of low-emission cost-effective dwellings. *Build. Environ.* **2011**, *46*, 109–123. [CrossRef]
30. Davidson, S. Grasshopper—Algorithmic Modeling for Rhino. Available online: www.grasshopper3d.com (accessed on 27 June 2015).
31. Gupta, C. A systematic approach to optimum thermal design. *Build. Sci.* **1970**, *5*, 165–173. [CrossRef]
32. Caldas, L.G.; Norford, L.K. A design optimization tool based on a genetic algorithm. *Autom. Constr.* **2002**, *2*, 173–184. [CrossRef]
33. Østergård, T.; Jensen, R.L.; Maagaard, S.E. Building simulations supporting decision making in early design—A review. *Renew. Sustain. Energy Rev.* **2016**, *61*, 187–201. [CrossRef]
34. Kheiri, F. A review on optimization methods applied in energy-efficient building geometry and envelope design. *Renew. Sustain. Energy Rev.* **2018**, *92*, 897–920. [CrossRef]
35. Holland, J.H. *Adaptation in Natural and Artificial Systems: An Introductory Analysis with Applications to Biology, Control, and Artificial Intelligence*; The MIT Press: Cambridge, MA, USA, 1992.
36. Zhang, L.; Wang, C.; Chen, Y.; Zhang, L. Multi-Objective Optimization Method for the Shape of Large-Space Buildings Dominated by Solar Energy Gain in the Early Design Stage. *Front. Energy Res.* **2021**, *9*, 744974. [CrossRef]
37. Lin, B.; Chen, H.; Yu, Q.; Zhou, X.; Lv, S.; He, Q.; Li, Z. MOOSAS—A systematic solution for multiple objective building performance optimization in the early design stage. *Build. Environ.* **2021**, *200*, 107929. [CrossRef]
38. Ochoa, C.E.; Aries, M.B.; Loenen, E.J.V.; Hensen, J.L. Considerations on design optimization criteria for windows providing low energy consumption and high visual comfort. *Appl. Energy* **2012**, *95*, 238–245. [CrossRef]
39. Nateghi, S.; Mansoori, A.; Moghaddam, M.A.E.; Kaczmarczyk, J. Multi-objective optimization of a multi-story hotel's energy demand and investing the money saved in energy supply with solar energy production. *Energy Sustain. Dev.* **2023**, *72*, 33–41. [CrossRef]
40. Trinh, H.T.M.K.; Chowdhury, S.; Nguyen, M.T.; Liu, T. Optimising flat plate buildings based on carbon footprint using Branch-and-Reduce deterministic algorithm. *J. Clean. Prod.* **2021**, *320*, 128780. [CrossRef]
41. Yi, Y.K.; Malkawi, A. Site-specific optimal energy form generation based on hierarchical geometry relation. *Autom. Constr.* **2012**, *26*, 77–91. [CrossRef]
42. Vermeulen, T.; Knopf-Lenoir, C.; Villon, P.; Beckers, B. Urban layout optimization framework to maximize direct solar irradiation. *Comput. Environ. Urban Syst.* **2015**, *51*, 1–12. [CrossRef]
43. Camporeale, P.E.; Mercader-Moyano, P. Towards nearly Zero Energy Buildings: Shape optimization of typical housing typologies in Ibero-American temperate climate cities from a holistic perspective. *Sol. Energy* **2019**, *193*, 738–765. [CrossRef]
44. Waibel, C.; Evins, R.; Carmeliet, J. Co-simulation and optimization of building geometry and multi-energy systems: Interdependencies in energy supply, energy demand and solar potentials. *Appl. Energy* **2019**, *242*, 1661–1682. [CrossRef]
45. Ekici, B.; Cubukcuoglu, C.; Turrin, M.; Sariyildiz, I.S. Performative computational architecture using swarm and evolutionary optimisation: A review. *Build. Environ.* **2019**, *147*, 356–371. [CrossRef]
46. Magnier, L.; Haghighat, F. Multiobjective optimization of building design using TRNSYS simulations, genetic algorithm, and Artificial Neural Network. *Build. Environ.* **2010**, *45*, 739–746. [CrossRef]
47. Giostra, S.; Masera, G.; Monteiro, R. Solar Typologies: A Comparative Analysis of Urban Form and Solar Potential. *Sustainability* **2022**, *14*, 9023. [CrossRef]
48. Ciardiello, A.; Rosso, F.; Dell, J.; Ciancio, V.; Ferrero, M.; Salata, F. Multi-objective approach to the optimization of shape and envelope in building energy design. *Appl. Energy* **2020**, *280*, 115984. [CrossRef]
49. Tuhus-Dubrow, D.; Krarti, M. Genetic-algorithm based approach to optimize building envelope design for residential buildings. *Build. Environ.* **2010**, *45*, 1574–1581. [CrossRef]
50. Nault, E.; Waibel, C.; Carmeliet, J.; Andersen, M. Development and test application of the UrbanSOLve decision-support prototype for early-stage neighborhood design. *Build. Environ.* **2018**, *137*, 58–72. [CrossRef]
51. Chen, K.W.; Janssen, P.; Schlueter, A. Multi-objective optimisation of building form, envelope and cooling system for improved building energy performance. *Autom. Constr.* **2018**, *94*, 449–457. [CrossRef]
52. EvoMass. Tutorials for Using the Rhino-Grasshopper Plugin EvoMass. 2022. Available online: https://www.youtube.com/playlist?list=PLjD0bF-7eaNgEfJrPQHiejlMTk2aQMRzO (accessed on 18 November 2022).
53. Wang, L.; Chen, K.W.; Janssen, P.; Ji, G. Enabling Optimisation-based Exploration for Building Massing Design—A Coding-free Evolutionary Building Massing Design Toolkit in Rhino-Grasshopper. In Proceedings of the 25th International Conference of the Association for Computer-Aided Architectural Design Research in Asia (CAADRIA), Bangkok, Thailand, 5–6 August 2020.
54. Luca, F.D.; Sepúlveda, A. Urban Shaderade. Building Space Analysis Method for Energy and Sunlight Consideration in Urban Environments. In *Communications in Computer and Information Science*; Springer: Berlin/Heidelberg, Germany, 2023; pp. 317–332.
55. Knowles, R.L. *Sun Rhythm Form*; MIT Press: Cambridge, MA, USA, 1981.
56. Evins, R. A review of computational optimisation methods applied to sustainable building design. *Renew. Sustain. Energy Rev.* **2013**, *22*, 230–245. [CrossRef]
57. Gagne, J.M.; Andersen, M. A Generative Façade Design Method Based on Daylighting Performance Goals. *J. Build. Perform. Simul.* **2012**, *5*, 141–154. [CrossRef]

58. Carlucci, S.; Cattarin, G.; Causone, F.; Pagliano, L. Multi-objective optimization of a nearly zero-energy building based on thermal and visual discomfort minimization using a non-dominated sorting genetic algorithm (NSGA-II). *Energy Build.* **2015**, *104*, 378–394. [CrossRef]
59. Jafari, A.; Valentin, V. Selection of optimization objectives for decision-making in building energy retrofits. *Build. Environ.* **2018**, *130*, 94–103. [CrossRef]
60. Ascione, F.; Bianco, N.; Mauro, G.M.; Vanoli, G.P. A new comprehensive framework for the multi-objective optimization of building energy design: Harlequin. *Appl. Energy* **2019**, *241*, 331–361. [CrossRef]
61. Gou, S.; Nik, V.M.; Scartezzini, J.-L.; Zhao, Q.; Li, Z. Passive design optimization of newly-built residential buildings in Shanghai for improving indoor thermal comfort while reducing building energy demand. *Energy Build.* **2018**, *169*, 484–506. [CrossRef]
62. U.S. Green Building Council. LEED Rating System. 2015. Available online: https://www.usgbc.org/leed (accessed on 7 July 2015).
63. Attia, S.; Hamdy, M.; O'Brien, W.; Carlucci, S. Assessing gaps and needs for integrating building performance optimization tools in net zero energy buildings design. *Energy Build.* **2013**, *60*, 110–124. [CrossRef]
64. Touloupaki, E.; Theodosiou, T. Performance Simulation Integrated in Parametric 3D Modeling as a Method for Early Stage Design Optimization—A Review. *Energies* **2017**, *10*, 637. [CrossRef]
65. Wortmann, T.; Cichocka, J.; Waibel, C. Simulation-based optimization in architecture and building engineering—Results from an international user survey in practice and research. *Energy Build.* **2022**, *259*, 111863. [CrossRef]
66. Kanters, J.; Horvat, M.; Dubois, M.-C. Tools and methods used by architects for solar design. *Energy Build.* **2014**, *68*, 721–731. [CrossRef]
67. Reinhart, C.F.; Davila, C.C. Urban building energy modeling—A review of a nascent field. *Build. Environ.* **2016**, *97*, 196–202. [CrossRef]
68. Batueva, E.; Mahdavi, A. Assessment of a computational design environment with embedded simulation capability. In Proceedings of the 10th European Conference on Product and Process Modelling (ECPPM2014); CRC Press: Vienna, Austria, 2014.
69. Baker, N.; Steemers, K. *Energy and Environment in Architecture: Technical Design Guide*; E & FN SPON: London, UK, 2000.
70. Wang, W.; Zmeureanu, R.; Rivard, H. Applying multi-objective genetic algorithms in green building design optimization. *Build. Environ.* **2005**, *40*, 1512–1525. [CrossRef]
71. Nault, E.; Peronato, G.; Rey, E.; Andersen, M. Review and critical analysis of early-design phase evaluation metrics for the solar potential of neighborhood designs. *Build. Environ.* **2015**, *92*, 679–691. [CrossRef]
72. Solomon, S.; Qin, D.; Manning, M.; Marquis, M.; Averyt, K.; Tignor, M.M.; Miller, H.L., Jr.; Chen, Z. (Eds.) *The Intergovernmental Panel on Climate Change, Climate Change 2007: The Physical Science Basis, Vol. Contribution of Working Group I to the Fourth Assessment Report of the Intergovernmental Panel on Climate Change*; Cambridge University Press: New York, NY, USA, 2007.
73. Dekay, M.; Brown, G.Z. *Sun, Wind, and Light: Architectural Design Strategies*; John Wiley & Sons: Hoboken, NJ, USA, 2014.
74. Zhao, S.; Angelis, E.D. Performance-based Generative Architecture Design: A Review on Design Problem Formulation and Software Utilization. *J. Integr. Des. Process Sci.* **2019**, *22*, 55–76. [CrossRef]
75. March, L.; Trace, M. *The Land Use Performances of Selected Arrays of Built Forms*; Centre for Land Use and Built Form Studies; University of Cambridge: Cambridge, UK, 1968.
76. Rode, P.; Keim, C.; Robazza, G.; Viejo, P.; Schofield, J.R. Cities and Energy: Urban Morphology and Residential Heat-Energy Demand. *Environ. Plan. B Plan. Des.* **2014**, *41*, 138–162. [CrossRef]
77. Makido, Y.; Dhakal, S.; Yamagata, Y. Relationship between urban form and CO_2 emissions: Evidence from fifty Japanese cities. *Urban Clim.* **2012**, *2*, 55–67. [CrossRef]
78. Pacific Northwest National Laboratory. *VOLUME 7.3 High-Performance Home Technologies: Guide to Determining Climate Regions by County*; U.S. Department of Energy: Washington, DC, USA, 2015.
79. Solemma. Climate Studio. 2022. Available online: https://www.solemma.com/climatestudio (accessed on 4 February 2023).
80. Yao, R.; Steemers, K. A method of formulating energy load profile for domestic buildings in the UK. *Energy Build.* **2005**, *37*, 663–671. [CrossRef]
81. *ASHRAE 90.1-2004*; Energy Standard for Buildings Except Low-Rise Residential Buildings. American Society of Heating, Refrigerating and Air-Conditioning Engineers, Inc.: Atlanta, GA, USA, 2007.
82. *ISO 17772:2017*; Energy performance of buildings. ISO: Geneva, Switzerland, 2017.
83. USGBC. Daylight. U.S. Green Building Council. Available online: https://www.usgbc.org/credits/healthcare/v4-draft/eqc-0 (accessed on 8 March 2024).
84. International Code Council. *International Building Code*; ICC Publications: Paris, France, 2021.
85. "Legislative Decree 3 March 2011, n. 28", 3 3 2011. Available online: https://www.gazzettaufficiale.it/eli/id/2011/03/28/011G0067/sg (accessed on 27 October 2021).
86. Vierlinger, R. Octopus. 2012. Available online: https://www.food4rhino.com/en/app/octopus (accessed on 12 August 2022).
87. Radford, A.D.; Gero, J.S. On optimization in computer aided architectural design. *Build. Environ.* **1980**, *15*, 73–80. [CrossRef]